




# Eemian landscape response to climatic shifts and evidence for northerly Neanderthal occupation at a palaeolake margin in northern Germany

Michael Hein<sup>1</sup>  | Brigitte Urban<sup>2</sup> | David Colin Tanner<sup>3</sup>  |  
 Anton Hermann Bunes<sup>3</sup> | Mario Tucci<sup>2</sup> | Philipp Hoelzmann<sup>4</sup> | Sabine Dietel<sup>5</sup> |  
 Marie Kaniecki<sup>1</sup> | Jonathan Schultz<sup>1,5</sup> | Thomas Kasper<sup>6</sup> |  
 Hans von Suchodoletz<sup>7</sup>  | Antje Schwalb<sup>8</sup> | Marcel Weiss<sup>9,1</sup> | Tobias Lauer<sup>1</sup>

<sup>1</sup>Department of Human Evolution, Max Planck Institute for Evolutionary Anthropology, Leipzig, Germany

<sup>2</sup>Institute of Ecology, Leuphana University of Lüneburg, Lüneburg, Germany

<sup>3</sup>Section 1: Seismic, Gravimetry, and Magnetism, Leibniz Institute for Applied Geophysics, Hannover, Germany

<sup>4</sup>Institute for Geographical Sciences, Freie Universität Berlin, Berlin, Germany

<sup>5</sup>Institute for Geosciences and Geography, Martin Luther University Halle-Wittenberg, Halle, Germany

<sup>6</sup>Institute for Geography, Friedrich Schiller University Jena, Jena, Germany

<sup>7</sup>Department of Geography, Faculty of Physics and Geosciences, University of Leipzig, Leipzig, Germany

<sup>8</sup>Institute of Geosystems and Bioindication, Technical University Braunschweig, Braunschweig, Germany

<sup>9</sup>Institut für Ur- und Frühgeschichte, Friedrich-Alexander-Universität Erlangen-Nürnberg, Erlangen, Germany

## Correspondence

Michael Hein, Department of Human Evolution, Max-Planck-Institute for Evolutionary Anthropology, Deutscher Platz 6, Leipzig, Saxony, 04103, Germany.  
 Email: michael\_hein@eva.mpg.de

Dr Marcel Weiss, Institut für Ur- und Frühgeschichte, Friedrich-Alexander-Universität Erlangen-Nürnberg, Kochstr. 4/18, Erlangen, Bayern, 91054, Germany.  
 Email: marcel.weiss@fau.de

## Funding information

Max-Planck-Gesellschaft

## Abstract

The prevailing view suggests that the Eemian interglacial on the European Plain was characterized by largely negligible geomorphic activity beyond the coastal areas. However, systematic geomorphological studies are sparse. Here we present a detailed reconstruction of Eemian to Early Weichselian landscape evolution in the vicinity of a small fingerlake on the northern margin of the Salzwedel Palaeolake in Lower Saxony (Germany). We apply a combination of seismics, sediment coring, pollen analysis and luminescence dating on a complex sequence of colluvial, paludal and lacustrine sediments. Results suggest two pronounced phases of geomorphic activity, directly before the onset and at the end of the Eemian period, with an intermediate period of pronounced landscape stability. The dynamic phases were largely driven by incomplete vegetation cover, but likely accentuated by fluvial incision in the neighbouring Elbe Valley. Furthermore, we discovered Neanderthal occupation at the lake-shore during Eemian pollen zone (PZ) E IV, which is chronologically in line with other known Eemian sites of central Europe. Our highly-resolved spatio-temporal data substantially contribute to the understanding of climate-induced geomorphic processes throughout and directly after the last interglacial period. It helps unraveling the landscape dynamics between the coastal areas to the north and the loess belt to the south.

## KEYWORDS

Eemian interglacial, landscape evolution, luminescence dating, Neanderthal occupation, paleolake, pollen analysis

## 1 | INTRODUCTION

Climate and environmental dynamics of the last interglacial, termed ‘Eemian’ in central and north-western Europe, have been studied more intensively on the European Plain than in any other region on Earth. This is largely due to the very frequent occurrence of Eemian geoarchives, in an area roughly equivalent to the maximum extent of the Saalian glaciation (Figure 1) (Turner, 2002; van Kolfschoten & Gibbard, 2000; Źarski et al., 2018). The vast majority of geomorphological studies focus on the loess belt (Antoine et al., 2016; Haesaerts & Mestdagh, 2000), riverine environments (Busschers et al., 2007; De Clercq et al., 2018; Gibbard & Lewin, 2002; Peeters et al., 2015), as well as the coastal areas that respond to Eemian sea level changes (Head et al., 2005; Höfle et al., 1985; Marks et al., 2014; Miettinen et al., 2014; Streif, 2004). Results of these studies suggest non-depositional, stable conditions with dominating pedogenesis during the temperate phases of the Eemian. The region in between the coasts and the loess belt, that is, the lowland landscapes remain underrepresented in this research. Nevertheless, this area hosts a multitude of mostly small isolated basins (diametres of a few decametres to some hundred metres), formed as kettle holes in the underlying Saalian till (Turner, 2000). These were formed at the end of the Saalian glaciation, when local depressions, caused by melting ice blocks (dead ice) enabled accommodation of usually lacustrine and paludal Eemian sediments. In the past decades, valuable information on the palaeoenvironmental and palaeoclimatic development of the Eemian has been retrieved from such archives (e.g., Behre et al., 2005; Björck et al., 2000; Kołaczek et al., 2016; Kupryjanowicz et al., 2018; Köhl et al., 2007; Menke & Tynni, 1984; Rother et al., 2019; Velichko et al., 2005). However, there are several disadvantages related to the small dimensions of these closed depressions, which affect the interpretation of past climate and vegetation variability, and particularly of geomorphic activity in response to environmental changes: (i) These landforms do not exclusively store information on climatic conditions, but their infills are also heavily affected by the very local hydrographic situation, likely to overprint the palaeoclimate signal (Turner, 2000;

cf. Vandenberghe & van der Plicht, 2016). (ii) Records derived from these archives are often discontinuous. This is one of the main reasons that a general agreement upon the exact timing and duration of the terrestrial Eemian is still pending (although it is generally correlated with Marine Isotope Stage [MIS] 5e) (see discussions in Brauer et al., 2007; Lisiecki & Raymo, 2005; Shackleton et al., 2002; Sier et al., 2015). (iii) Their minor extent and small-sized catchment areas do generally not allow statements about regional geomorphic landscape dynamics. Consequently, it is still not clear, how inland lowland landscapes of the European Plain responded to Eemian environmental changes.

Therefore, detailed information on the Eemian landscape dynamics in the lowlands can only be obtained by studying sedimentary basins that offer larger accommodation space compared to the small closed depressions, testifying to both, temporally and spatially varying sedimentation processes. In this study, we investigate sediments of a palaeolake margin adjacent to the Elbe ice-marginal valley to assess the Eemian landscape evolution of the northern German lowlands between the coasts in the north and the loess belt and low-mountain ranges in the south. By using a borehole transect, seismic surveys and palynology, we decipher the geomorphic, vegetation and sedimentary history of this area from the Late Saalian until the Early Weichselian period with a high spatio-temporal resolution.

## 2 | STUDY AREA

The study site is situated near the village of Lichtenberg in eastern Lower-Saxony, northern Germany (Figure 2). In the course of the Pleistocene, this area was formed by alternating glacial, periglacial and interglacial/interstadial conditions. Glaciers covered the area at least twice during the Elsterian glaciation (MIS 12) and three times during the Saalian glaciation (MIS 6, stages Drenthe I, Drenthe II and Warthe), depositing > 40 m of tills, glaciofluvial sands and gravels in total (Duphorn et al., 1973; Ehlers et al., 2011; Lang et al., 2018; Stephan, 2014). These glacial sediments are found in the echeloned

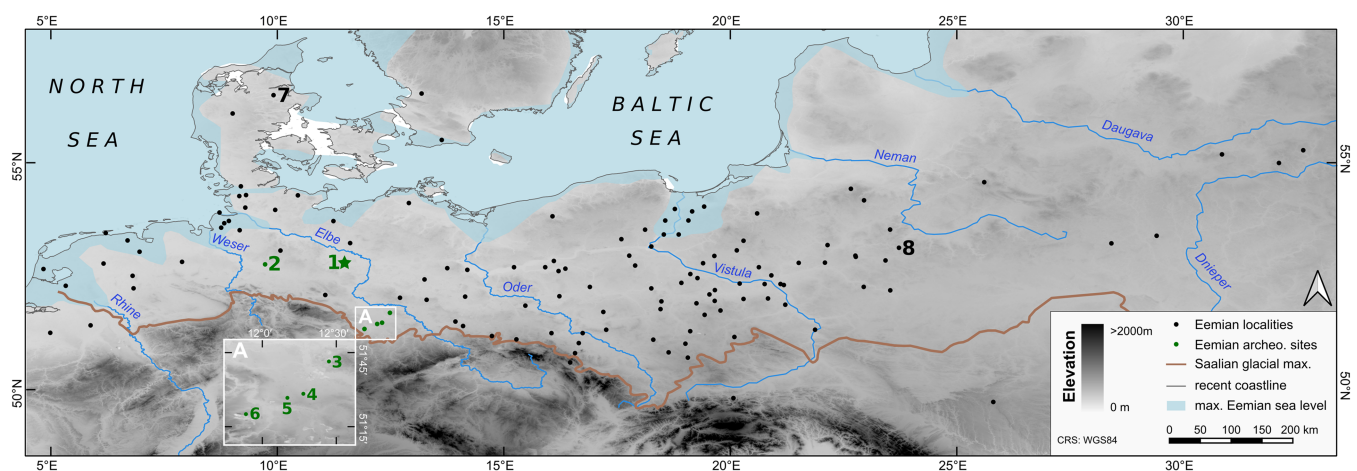


**FIGURE 1** Digital elevation model (DEM) of the European Plain, showing the maximum Saalian ice margins (after Ehlers et al. [1984], Matoshko [2011] and Velichko et al. [2006]) and selected localities of Eemian deposits (compiled from Kołaczek et al. [2016], Turner [2000] and Velichko et al. [2005]). Eemian sea-level highstands after Miettinen et al. (2014). Sites mentioned in the text: 1, Lichtenberg; 2, Lehringen; 3, Gröbern; 4, Grabschütz; 5, Rabutz; 6, Neumark-Nord; 7, Hollerup; 8, Jalówka. Localities marked in green are also archeological sites. DEM based on SRTM-data (downloaded from <https://earthexplorer.usgs.gov/>), river courses are from open streetmap data, obtained from <http://download.geofabrik.de/europe.html> [Color figure can be viewed at [wileyonlinelibrary.com](http://wileyonlinelibrary.com)]

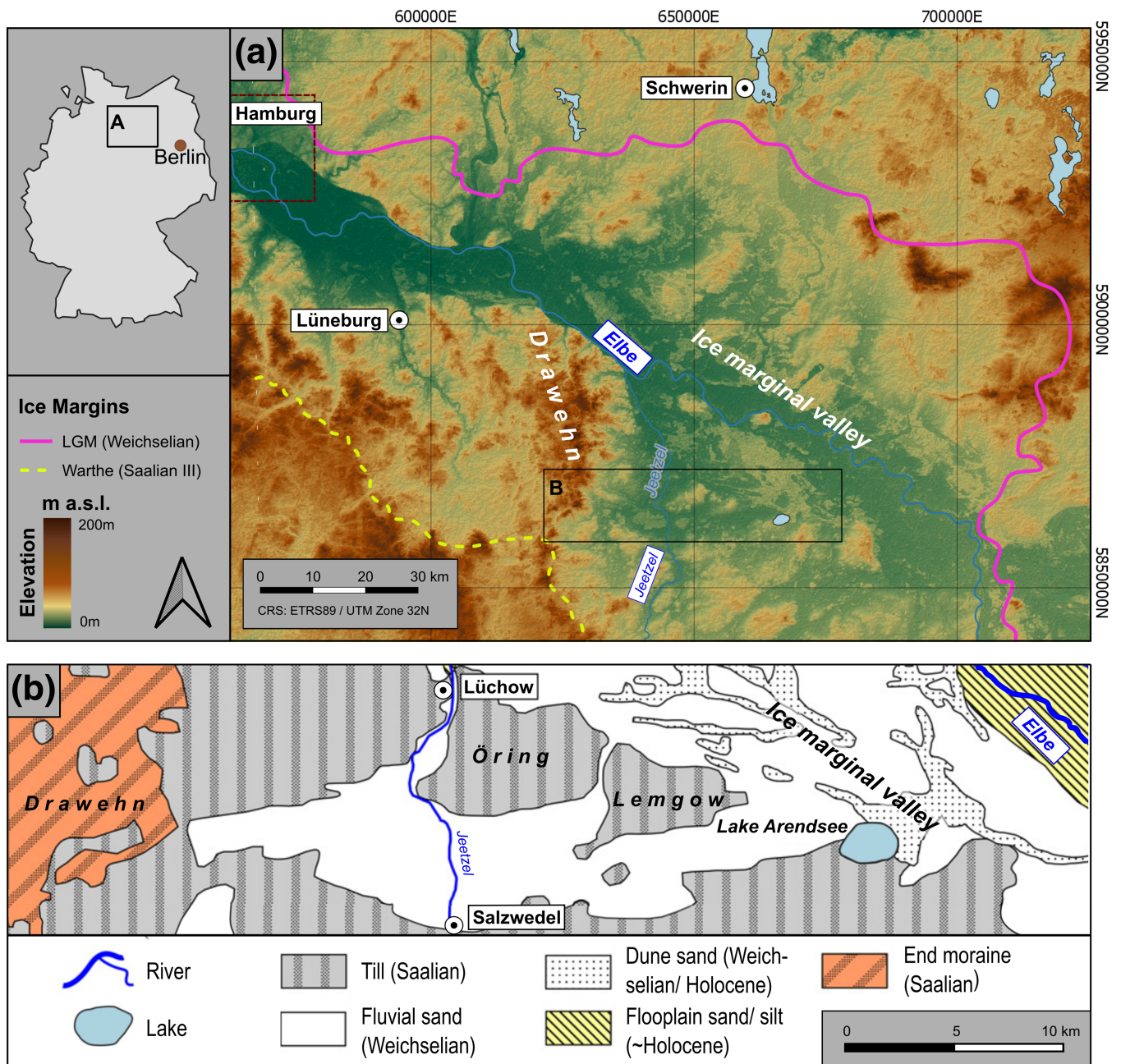


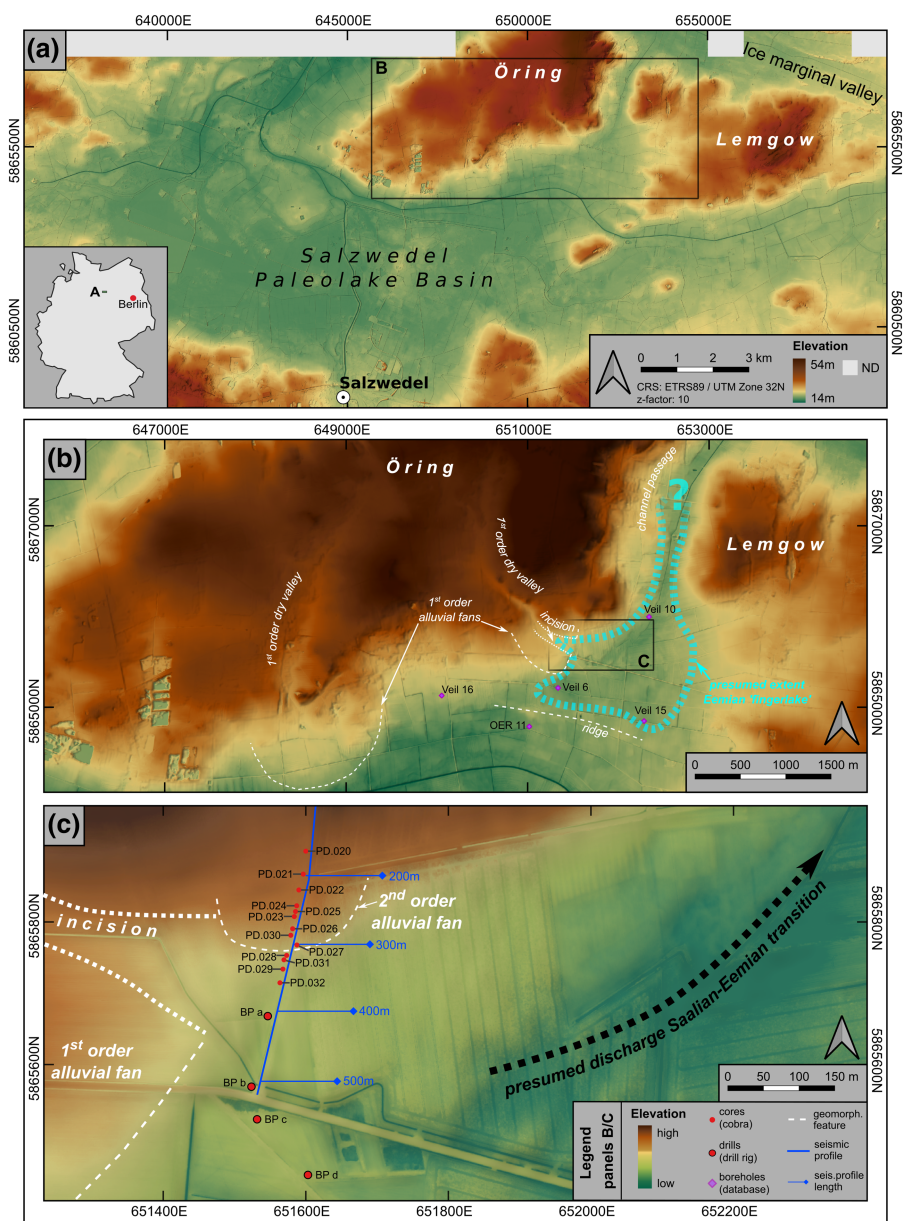
**FIGURE 2** (a) Location map of the study area in northern Germany based on an SRTM-DEM (obtained from <https://earthexplorer.usgs.gov/>). Ice margins according to Ehlers and Gibbard (2004), river courses downloaded from <http://download.geofabrik.de/europe.html>. (b) Quaternary geology of the study area, modified after Turner et al. (2013) [Color figure can be viewed at [wileyonlinelibrary.com](http://wileyonlinelibrary.com)]

retreat moraine of the Drawehn (Figure 2) and as solitary inliers of morainic hills (e.g., Öring and Lemgow) within genetically-younger lowland areas (Merkt, 1975; Voss, 1981). In contrast, the region and study area remained unglaciated throughout the Weichselian glaciation (MIS 4 to MIS 2), with the Last Glacial Maximum (LGM) ice margin located c. 50 km to the northeast (Figure 2a). The associated ice-marginal valley is now partly occupied by the recent River Elbe, but it covered more extensive areas (Meyer, 1983; Woldstedt, 1956), so that it delimits the Öring and Lemgow to the north (Figures 2 and 3). The Eemian course of the lower Elbe has been highly debated in the past, in particular the time at which the river occupied its current position following the Saalian glaciations (Illies, 1954; Lüttig & Meyer, 1974; Woldstedt, 1956). However, it is now widely accepted

that the ice-marginal valley formed even prior to the late Saalian Warthe Stadial and attracted the regional discharge from this time onward (Averdieck, 1976; Ehlers, 1990; Grube et al., 1976; Meyer, 1983). Significant subsidence around the Elbe tectonic lineament is thought to have been an important factor in its evolution (Brandes et al., 2019; Reicherter et al., 2005). At least since the end of the Warthe Stadial, the connection to the upper Elbe reaches in Saxony and Bohemia was established, so that a general congruence of the Eemian, the Weichselian and Holocene courses can be assumed (Ehlers, 2020).

The study site is located within the lowlands south of Öring and Lemgow, extending between Lake Arendsee and Jeetzel River (Figure 2b). Veil et al. (1994) first proposed this depression might once have contained a palaeolake (Figure 3a). This assumption was

**FIGURE 3** Digital elevation models (DEMs) of the study area showing geomorphic features and the positions of the seismic and borehole profiles. Descriptions in the text, Section 2 and Supporting Information Method S1. Core descriptions of previous studies found in the borehole database of Lower Saxony (<https://nibis.lbeg.de/cardomap3/>). For the geological cross-section (P1–P2) in (A), see Supporting Information Figure S1 [Color figure can be viewed at [wileyonlinelibrary.com](https://onlinelibrary.wiley.com)]



based on the size and rhomboid shape of the basin and the fine-grained sediment infill, as documented in the borehole database of the State Office for Mining, Energy and Geology, Lower Saxony (<https://nibis.lbeg.de/cardomap3>). Hereafter, we refer to this basin as ‘Salzwedel Palaeolake’ (named after the largest adjacent city). Moreover, Veil et al. (1994) discovered paludal and lacustrine residues at the basin margin, possibly associated with this palaeolake. By using biostratigraphic assumptions, these deposits were dated to the Eemian and the early MIS 4 (*ibid.*), suggesting a permanent body of water at the time of their sedimentation. Our investigations were carried out on the northern margin of Salzwedel Palaeolake, at the eastern scarp of an alluvial fan, discernible as a current geomorphic feature. In this fan, a slight elongated and west–east striking depression indicates a former incision into this landform, thereby creating a sedimentary basin, which is the subject of this study. Lengthwise, the borehole transect also cuts a smaller (second order) alluvial fan, cast into this basin. Additional information on the local geomorphological situation is given in Section 5.2 and Supporting Information Method S1.

### 3 | METHODS

#### 3.1 | Fieldwork

Coring campaigns were conducted in 2019 and 2020 within the framework of an ongoing geoarchaeological research project on the Middle-Palaeolithic occupation of the Lichtenberg site (Veil et al., 1994; Weiss, 2020) and meant to provide palaeoenvironmental context for that period. Hence, fieldwork comprised also an archaeological survey. The basin infill sequence was exposed by a > 600 m long transect of 20 boreholes (16 vibrocores, down to 11 m and four rotary drills, down to 21 m), carried out perpendicular to the orientation of the basin, at carefully chosen locations (for core positions see Figures 3c and 4). The vibrocores were drilled with an *Atlas Copco Cobra* motor hammer using open probes of 1 m length and 50 to 80 mm diameter. Rotary drilling was conducted in cooperation with the State Office for Mining, Energy and Geology of Lower-Saxony (LBEG), utilizing a truck-mounted drill-rig and 3 m augers with c. 25 cm diameter. The average recovery rate for the continuous cores

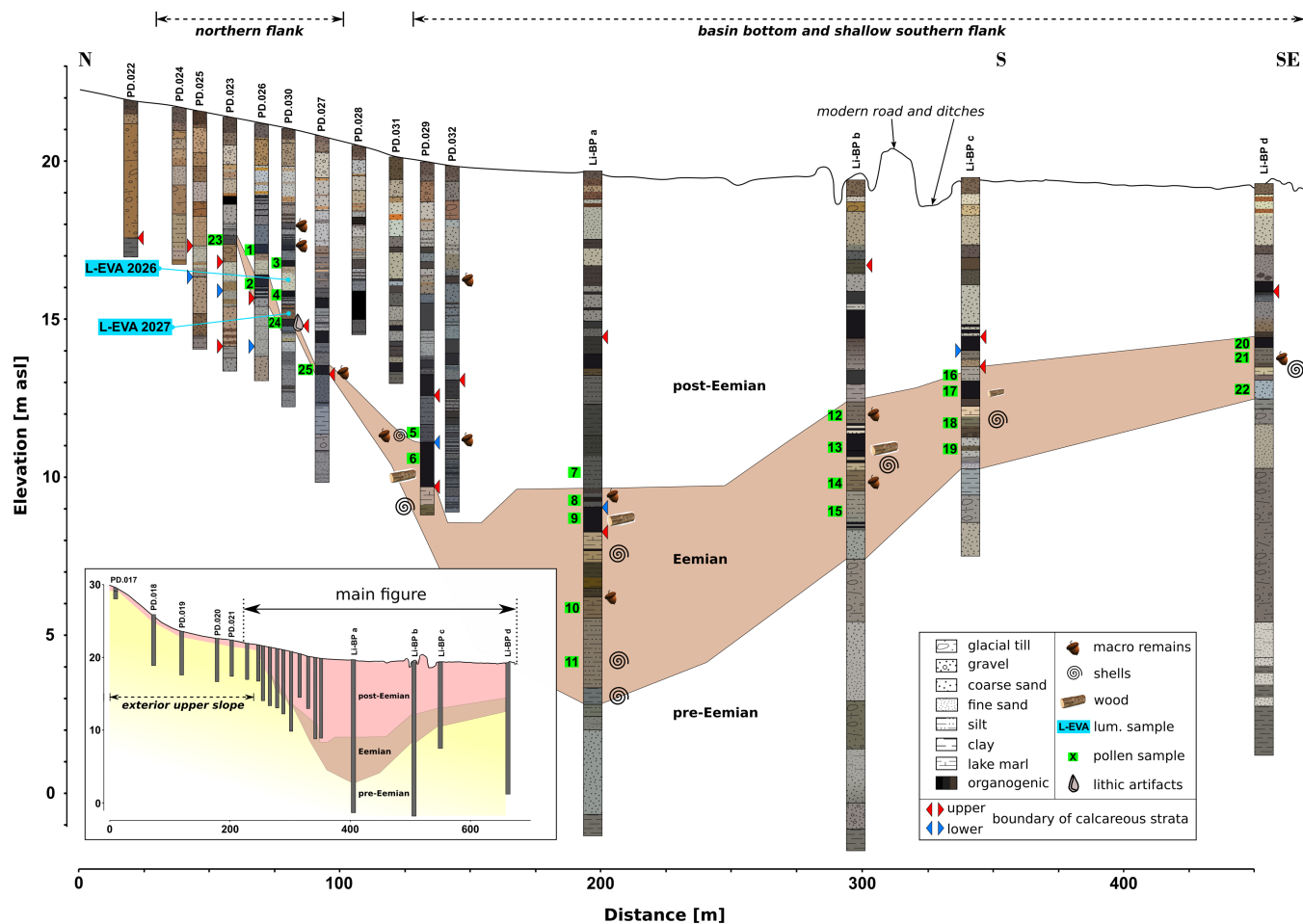


**FIGURE 4** Sedimentary log of the borehole transect along with the positions of luminescence and pollen sampling (samples for organic carbon ( $C_{org}$ ) and nitrogen (N) measurements taken from the pollen batch). Colouring of the cores corresponds with the MUNSELL colours, ascribed during fieldwork. Vertical exaggeration 1:12. For borehole logs of the exterior upper slope, see Supporting Information Figure S4 [Color figure can be viewed at [wileyonlinelibrary.com](http://wileyonlinelibrary.com)]

was always > 90%. Sediment descriptions in the field encompassed sediment boundaries, MUNSELL colours, admixtures (such as gravels, botanical macro remains, charcoal, shell fragments), grain-size compositions and carbonate contents, and followed the German soil mapping guidelines of Boden (2005). Organogenic sediments were classified according to Meier-Uhlherr et al. (2015). Subsequently, selected sediment units were sampled for luminescence dating, palynological analyses, and measurements of organic carbon and nitrogen content (Sections 3.3–3.5, Figure 4).

### 3.2 | S-wave seismic reflection

In alignment with the coring transect, we measured a seismic S-wave profile of 520 m length. We used a small electrodynamic vibrator (Elvis 7, Krawczyk et al., 2012) with a sweep frequency of 20 to 160 Hz. The 16 s sweep was excited perpendicular to the line direction at each shotpoint twice with opposite polarity and subtractively stacked to suppress P-wave energy. Recording was done using a landstreamer with 120 horizontally-oriented 10 Hz geophones. We worked in a symmetrical split-spread fashion by shooting 60 m to the middle of the streamer before moving it for the same distance. To maximize the seismic fold at the targeted layers we used a shotpoint spacing of 2 m, so that the corresponding common depth point (CDP)

fold was 31. Details on the processing of the seismic data are given in Supporting Information Table S1, additional methodological information is provided in Method S3.

### 3.3 | Palynological analysis

Twenty-five samples of characteristic lithological units/horizons were taken from nine drilled cores (PD.023, PD.026, PD.027, PD.029, PD.030, Li-BPa, Li-BPb, Li-BPc, Li-BPd) for palynological investigation and biostratigraphic determination (Figure 4). By taking bulk samples distributed across the entire borehole transect, we deliberately traded chronological resolution and unambiguity of pollen zone classification against higher spatial coverage in order to focus on the reconstruction of geomorphic dynamics. In about 10 g of wet sediment per sample, carbonates were removed first with 10% hydrochloric acid (HCl). The samples were then treated using standard methods (Faegri et al., 1989; Moore et al., 1991). The extracted residues were mounted in glycerine. Generally, one slide (24 mm × 32 mm) per sample was analysed under a transmitted light microscope for pollen and non-pollen palynomorphs at 40× magnification. Pollen and spores were identified using the atlases of Faegri et al. (1989), Moore et al. (1991) and Beug (2004), as well as the reference collections of the Palynology Laboratory of the

Institute of Ecology, Working Group Landscape Change, Leuphana University of Lüneburg, Germany.

The pollen sums, on which percentages of all taxa are based, were constructed by summing up arboreal pollen (AP), including trees and shrubs, and non-arboreal pollen (NAP), composed of terrestrial herbaceous taxa and Poaceae. In contrast, taxa from cryptogams, Ericaceae, Cyperaceae and aquatic plants were excluded from the basic sums. Pollen percentages were calculated and plotted using the software package TILIA (Grimm, 1990).

### 3.4 | pIRIR<sub>290</sub> luminescence dating

To complement the biostratigraphical age control provided by palynological analysis, we dated two samples (L-EVA 2026 and 2027) from core PD.030 using luminescence dating (see Figures 4 and 6 for sampling positions). Sample L-EVA 2027 was taken from an unstratified sand layer overlying an Eemian half-bog. A peat deposit covers this layer and is in turn overlain by a well-stratified gleyic medium sand, from which sample L-EVA 2026 was obtained. We carefully removed c. 1 cm of the outer material that was previously exposed to light and sampled 15 cm sections of the innermost sediment for luminescence (=  $D_e$ -samples) (cf., Nelson et al., 2019). The discarded outer material was added to the dose rate samples (Table S3), otherwise taken within

15 cm below and above the  $D_e$ -samples. Sample preparation and  $D_e$ -measurements on coarse-grained potassium-feldspar (125–180  $\mu\text{m}$ ) were conducted at the MPI-EVA, Leipzig, using the pIRIR<sub>290</sub> approach proposed by Thiel et al. (2011; cf., Hein et al., 2020). Detailed information on the data evaluation can be found in Method S4.

### 3.5 | Analyses of organic carbon and total nitrogen

To support the classification of different organogenic deposits, the contents of organic carbon ( $C_{\text{org}}$ ) and total nitrogen (TN) in pollen samples 2, 6, 8, and 23–25 (Figure 4) were determined by applying the methods and equipment described in Vogel et al. (2016). The  $C_{\text{org}}$  was treated both as a discrete parameter and to calculate the molar C/N ratio, the latter used to assess the decomposition rate of organic matter in soils (e.g., Högberg et al., 2006).

## 4 | RESULTS AND INTERPRETATION

### 4.1 | Infill stratigraphy

The coring transect across the morphological depression revealed a c. 500 m wide sedimentary basin. It contains a complex succession of

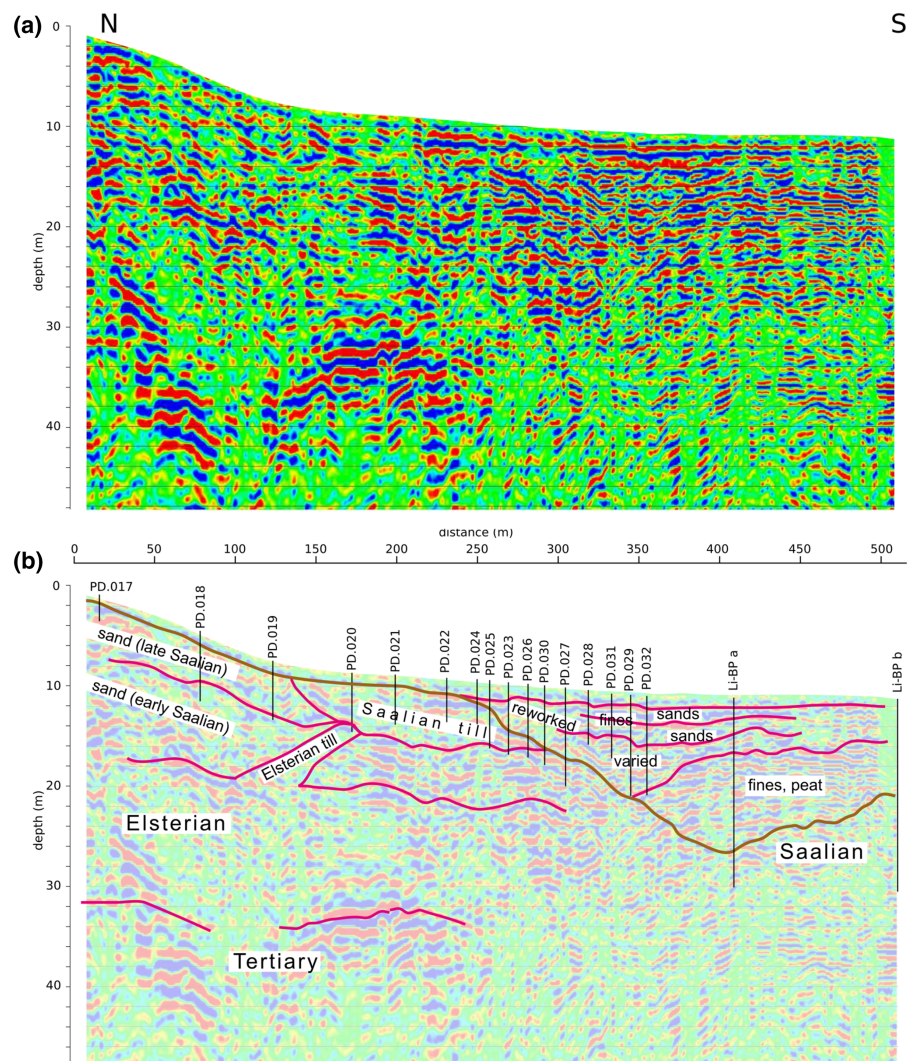


**FIGURE 5** (a) S-wave seismic profile with (b) interpretations [Color figure can be viewed at [wileyonlinelibrary.com](http://wileyonlinelibrary.com)]



**FIGURE 6** (a) Section 450 cm to 650 cm of core PD.030 with segments chosen for luminescence samples and the stratigraphic position of the artefacts. (b) Photographs of the artefacts LIA-86 and LIA-187, obtained from this core [Color figure can be viewed at [wileyonlinelibrary.com](http://wileyonlinelibrary.com)]

stacked organogenic, sandy, silty and loamy deposits, with varying hydromorphic features, and contents of organic matter and carbonates (Figure 4). For this study, we exclusively focus on the Eemian sediments; post-Eemian successions will be targeted in future studies. Our descriptions and correlations of sediment units in the field are based on three general chronological presumptions:

- i. The basin was created during the Saalian-Eemian transition (cf., Fränzle, 1988; Garleff & Leontaris, 1971, and Method S1).
- ii. Organic-rich layers relate to temperate intervals (interglacials/interstadials), whereas less organic clastic deposits represent glacials and stadials.
- iii. Following (i) and (ii), the lowermost organic-rich limnic-paludal basin infill is assumed to be of Eemian age (Veil et al., 1994).

To achieve the best spatio-temporal coverage and the utmost information for this time-period, the pollen samples were distributed across all assumed Eemian deposits along the transect (Figure 4).

The S-wave seismic profile and the borehole information complement each other well and their mutual interpretation allows sediment-body boundaries to be laterally extended (Figure 5b). According to geomorphic position, thickness and characteristics of the post-Saalian sediments, we divided the borehole transect into three different sections: (i) the exterior upper slope, located outside of the basin ('exterior'), (ii) the steep northern flank of the basin ('northern flank') and (iii) the bottom and shallow southern flank of the basin ('bottom section') (Figure 4). Next, the respective lithological and seismic properties of these three sections are presented and described.

#### 4.1.1 | Exterior upper slope (cores PD.017 to PD.022)

The exterior part of the transect encompasses the cores PD.017 to PD.022 (Figures 4, 5b and Supporting Information Figure S4). They mainly expose Saalian glacial deposits, as also confirmed by the geological map (1:25000, number 3033 [Merkt, 1975]) and a nearby geological cross-section of the Öring (Figure S1). Between cores PD.017 and PD.019, the steeper slope corresponds with non-calcareous, well-stratified fine to coarse Saalian glaciofluvial sands. These are characterized by mildly reflective and discontinuous seismic reflectors that dip southwards in unison with the current topography (Figure 5). Southwards from core PD.019, the topography flattens out and Saalian glacial tills, partly associated with glacio-limnic clays appear. Their thickness increases to the south and reaches > 5 m in cores PD.021 and 022. Even at such depths, the tills and clays are deeply weathered and decalcified. In PD.020, at 420 cm depth, an Elsterian till was encountered, distinguished from the Saalian tills mainly by its blackish-grey colour caused by lignite-uptake of the Elsterian glaciers (cf. Voss, 1981, Figures S1 and S4). Seismic reflections suggest that it represents an intercalation rather than the surface of a continuous Elsterian sediment body (Figure 5). Other than this, the presumed top of the Elsterian is continuous and highly reflective, but the respective till quickly loses reflectivity downwards, so that its base is near transparent in the seismic data. Seismic reflectors of this sediment are generally short, less than 20 m in length. Similar to the Saalian sediments, the Elsterian material dips in accordance with the present topography. The upper Tertiary boundary is interpreted to occur below 30 m

depth, where strong reflections start. These reflectors are of long wavelength, continuous over 40–100 m and they slightly arcuate upwards. This surface can only be followed to 250 m distance in the seismic profile; it fades out directly underneath the infilled basin above (Figure 5). The glacial sediments in the exterior section are overlain by shallow (< 2 m), gravelly Weichselian slope deposits (cf., Veil et al., 1994), generated by alternating solifluction and slope wash processes. These layers continue to form the uppermost part of all the cores along the rest of the borehole transect.

#### 4.1.2 | Northern flank (cores PD.024 to PD.027)

Both, seismic and borehole data document a basin opening up to the south, which created accommodation space to trap complex post-Saalian deposits. The base of this basin is formed by a rather steep, south-facing disconformity. In the seismic profile, this erosive surface is highly reflective itself and correlates very well with the lithology of the boreholes, showing the transition from glacial sediments to fine-grained deposits. This section includes the stretch between cores PD.024 and PD.027, while the neighbouring cores PD.028 and PD.031 are too shallow to penetrate Eemian or even Saalian glacial sediments. In cores PD.024 to PD.023, the Saalian glacial till, found in the previous exterior section still underlies the infill deposits. However, it thins out to the south until it vanishes from core PD.026 southwards, presumably due to erosion. The lowermost organic-rich layers were interpreted as Eemian and are aligned with the disconformity, and hence they dip at a sharp angle. These layers comprise 25 to 35 cm-thick, strongly organic sands (half-bog soils), and certainly developed due to water-logging or a high groundwater table. This material is devoid of carbonates, with the decalcification boundary mostly situated directly underneath (Figure 4). An exception is the loamy segment 370–400 cm in core PD.023. It is much less humic and decalcification has affected and weathered 60 cm of the underlying Saalian till, as well. This segment is thus described as a terrestrial topsoil horizon, seemingly unimpacted by hydromorphic processes during its development (see Method S5).

The assumed post-Eemian deposits show alternating sequences of peat/muds and well-bedded medium sands, which are interpreted as niveo-fluviatile slope deposits (cf. Veil et al., 1994). Chaotic seismic reflections between cores PD.023 and PD.027 ('reworked' in Figure 5b) may correspond with higher-energy short-distance reworking of sediments in the middle part of these cores. The occurrence of this phenomenon is congruent with the present morphological extent of the second order alluvial fan and was therefore cautiously attributed to its formation (Figures 3b,c and S3).

#### 4.1.3 | Bottom section (cores PD.029 to Li-BPd)

This section encompasses the flat bottom and the shallow north-facing slope of the basin. Its lower boundary shows only faint reflectivity in this part, but can still confidentially be correlated with the borehole information (Figure 5b). The lowermost fine-grained and organogenic deposits directly above the Saalian basement differ from those on the opposite flank with regards to thickness and properties, mainly due to different geomorphological and hydrological parameters

in a more aquatic setting with higher accommodation space. With a total thickness of 6 m, core Li-BPa captures the longest and most complete, supposedly Eemian sediment suite. At its base (17.3 to 15 m), a calcareous, clayey-silty sequence is found. Given the high amounts of organic matter and ubiquitous mollusk shells, these layers are classified as Eemian lacustrine sediments. The fines grade upwards into organic-enriched lake marls with intercalating detrital muds that are found between 15 and 13.4 m. Above (between 13.4 and 12.4 m), the marls appear as pure primary carbonate precipitations. These lake sediments are overlain by a 60 cm thick decalcified forest peat with large wood fragments. Upwards, the peat interfingers with calcareous silt, which eventually becomes dominant. Being in superposition of the lowest peat in the record, this silt might already mark the transition to the first Weichselian interstadial.

In cores PD.029 and Li-BPb to Li-BPd, quite similar sequences of peat and lake marls with varying thicknesses were observed across the suggested Eemian zone. However, towards the south, the basal silts known from Li-BPa are gradually substituted by sandy deposits. In addition, the peat in the southernmost core (Li-BPd) lacks wood fragments, implying a possible disparate formation process/time (see Section 5.1). Notably, most bottom deposits of this section are highly calcareous, except for the forest peat layers in cores Li-BPa and PD.029. This suggests a more acidic environment during the peat development. Within this section of the basin, the seismic data show high-amplitude reflectors up to 200 m long, where organogenic deposits alternate with silt in the lower parts and stratified sands in the upper parts of the cores. Especially in the fines and peat deposits, this alternation results in continuous, horizontal and highly reflective layers. However, north of core Li-BPa, oblique, northwards-dipping seismic phases and an area of less well-structured reflections ('varied' in Figure 5b) indicate an incision or reworking phase. This is corroborated by findings in core PD.032. Here, despite its close proximity to core PD.029, deep peat deposits are absent, even at 11 m depth. Instead, we encountered the same silty deposits that were documented above the forest peat in Li-BPa and that we interpreted as Early Weichselian. This suggests the peat had been eroded by this renewed incision.

Unfortunately, the structure below the basin is not visible in the seismic data. The boreholes, however, clearly and consistently show two Saalian calcareous glacial tills. These are detached from one another by thick bodies of glaciofluvial sands and show a basal glacio-lacustrine clay around an absolute elevation of 0 to 2 m above sea level (a.s.l.) (Figure 4, cf. Figure S1). Only at the position of core Li-BPa, these tills are missing, indicating erosion upon the formation of the basin. Nevertheless, it is apparent that the top of the upper till (visible in cores Li-BPb to Li-BPd and PD.027) created a slight depression, even before the basin formed.

## 4.2 | Palynology and biostratigraphy

Of the 25 analysed samples, two showed a very low pollen abundance (samples 19 and 23) and were hence rejected from interpretation. The remaining samples are presented and described in Table 1 and Figure S5. For the subdivision of the Eemian and the correlation of the pollen data, we refer to the description of Eemian pollen zones for north-western Germany by Menke and Tynni (1984) and to Behre



TABLE 1 Results of palynological analysis and geochemical proxies ( $C_{org}$ , C/N-ratio)

Sam-ple	Core	Depth (cm)	Lithology	Main pollen characteristics	Pollen zones/biostratigraphy (Menke & Tynni, 1984)	AP (%)	$C_{org}$ (%)	C/N
23	PD.023	370–390	humic loam	pollen-sterile	–	–	0.62	8.0
1	PD.026	400–410	sandy mud	poor in pollen, only <i>Betula</i>	tentative WF II	–	1.31	18.0
2	PD.026	480–490	peat	<i>Pinus</i> 88%, <i>Betula</i> 8%	E II/(E VII)	97.0	15.6	16.1
25	PD.027	730–765	half-bog peat	<i>Quercus-Carpinus</i> forest to <i>Pinus-Picea</i> ( <i>Abies</i> ) forest*	EV to E VI	–	7.41	23.7
3	PD.030	510–525	mud	<i>Betula</i> , <i>Pinus</i>	tentative WF II	94.4	1.23	13.9
4	PD.030	525–540	sandy peat	50% AP, 50% NAP, heliophytes	tentative WF I	54.5	13.4	15.5
24	PD.030	620–630	half-bog peat	<i>Corylus</i> , <i>Tilia</i> , <i>Carpinus</i>	E IV to E V	97.0	4.92	25.6
5	PD.029	745–770	humic silt/silty mud	Reworked pollen, glaciolimmic genesis, similar to sample 6	indifferent, (reworked)	88.5	6.63	17.6
6	PD.029	882–1,030	forest peat	<i>Pinus</i> , <i>Picea</i> , <i>Abies</i> , <i>Carpinus</i> , <i>Alnus</i>	EV to E VI	100	29.5	21.7
7	Li-BPa	900–1,025	humic silt	reworked from preceding Eemian PZ and glaciolimmic material	deposited during E VII/WF I?	97.2	9.8	20.7
8	Li-BPa	1,060–1,100	forest peat	bad preservation ( <i>Pinus</i> , <i>Betula</i> , <i>Picea</i> )	E VI (?)	96.0	19.5	24.6
9	Li-BPa	1,100–1,140	peat	<i>Pinus</i> , <i>Picea</i> , <i>Abies</i>	E VI	98.8	–	–
10	Li-BPa	1,340–1,415	lake-marl	<i>Pinus</i> , <i>Betula</i> , <i>Corylus</i> , <i>Quercus</i>	E IV	97.8	–	–
11	Li-BPa	1,500–1,625	silt, mollusks	reworked pollen, glaciolimmic genesis, similar sample 8	late Saalian/early E I?	89.9	–	–
12	Li-BPb	640–780	silt	reworked pollen from PAZ E6 and glaciolimmic input	reworked from late Eemian?	93.4	–	–
13	Li-BPb	800–850	peat	<i>Pinus</i> , <i>Picea</i> , <i>Carpinus</i> , <i>Abies</i>	E VI	97.4	–	–
14	Li-BPb	930–985	humic marl	<i>Corylus</i> peak, <i>Tilia</i> , <i>Quercus</i>	E IVb	99.7	–	–
15	Li-BPb	985–1,090	silt	<i>Corylus</i> , <i>Quercus</i> , <i>Carpinus</i> , <i>Betula</i> (50% local?), heliophytes, some reworked from glaciogenic input	tentative E IV	86.3	–	–
16	Li-BPc	600–640	silt	<i>Pinus</i> , <i>Picea</i> , <i>Abies</i>	E VI	97.5	–	–
17	Li-BPc	640–700	peat	<i>Carpinus</i> , <i>Picea</i> , <i>Corylus</i>	EV	99.2	–	–
18	Li-BPc	760–825	humic marl	<i>Carpinus</i> , <i>Corylus</i> , <i>Quercus</i> , <i>Ulmus</i> , <i>Tilia</i> , <i>Taxus</i>	EV	100	–	–
19	Li-BPc	870–900	humic sand	poor in pollen	not determined	–	–	–
20	Li-BPd	480–510	sandy peat/detritus	bad preservation, 60% <i>Pinus</i> , 27% <i>Betula</i>	E VII/(WF IIb)	90.1	–	–
21	Li-BPd	570–580	organic mud	<i>Carpinus</i> , <i>Alnus</i> , <i>Tilia</i> , <i>Picea</i> , few reworked pollen (glaciolimmic origin)	EV	96.8	–	–
22	Li-BPd	620–680	humic sand	<i>Corylus</i> peak (47%), <i>Quercus</i> , <i>Alnus</i> , <i>Taxus</i>	E IVb	96.6	–	–

AP, percentage of arboreal pollen;  $C_{org}$ , organic carbon; C/N, carbon/nitrogen ratio.

and Lade (1986). Local references are previous biostratigraphic results of an Eemian/Early Weichselian sequence from Lichtenberg (Veil et al., 1994) and yet unpublished data acquired by the authors. The amount of arboreal pollen is clearly above 85% for all samples but sample 4 (54.5%). Classification for nearly half of the samples was straightforward, based on the unambiguous taxa assemblage (samples 8–9, 13–14, 16–19, 21–22) (Table 1). The results completely confirm our sampling design and the preliminary interpretation of the deepest organogenic deposits as Eemian (see Section 4.1). However, our dispersed sampling approach in some instances made the assignment of certain palynomorph spectra to distinct pollen zones challenging, as longer sequences are lacking. In these cases, we proceeded as outlined in Method S2.

### 4.3 | Luminescence ages

The two pIRIR<sub>290</sub> ages are presented in Table 2 along with the  $1\sigma$  errors and the overdispersion (OD) values. Sample L-EVA 2027 was taken from an unstratified sandy layer directly above an Eemian half-bog, and has an age of  $104.6 \pm 10.5$  ka and an OD value of  $26.6 \pm 0.8\%$ . Sample L-EVA-2026 taken from a well-bedded sand at a higher stratigraphic position gave an age of  $108.4 \pm 17.0$  ka and an OD of  $33.3 \pm 1.4\%$ . The  $D_e$ -estimation and the robustness of the ages are discussed in Method S4.

### 4.4 | Geochemical proxies

The values for  $C_{org}$  and C/N confirm the field-based sedimentological findings (Table 1). The  $C_{org}$  varies between 0.62 (sample 23) and 29.5% (sample 6), while the C/N-ratio ranges between 8.0 (sample 23) and 25.6 (sample 24). Interpretations of these values with respect to field descriptions can be found in Method S5.

### 4.5 | Archaeological finds

In the sandy Eemian half-bog of core PD.030 (6.20 m depth), we recovered a longitudinal broken flake of Baltic flint with characteristics of a knapped lithic artefact (LIA-86, Figure 6b). The find layer is delimited by loamy Saalian sediments below, and complex, presumably pedogenetically-altered Weichselian sands above. To validate the hypothesis of a potential Eemian find concentration, we retrieved four additional cores within a 2 m radius. In this way, we recovered another flake (LIA-187, Figure 6b) and a number of undetermined small chips and fragments. In terms of a specific Middle Palaeolithic technology, the flakes are rather undiagnostic. The limited sample size of  $n = 2$  prevents any interpretation or attribution to a specific techno-complex. LIA-86 has a plain dorsal surface, and due to the

heavy dark patination, it is not clear whether this is an artificial surface resulting from a former flake removal or a natural surface. Additionally, the distal dorsal part has small recent damage from the drill. However, the right lateral edge consists of the former core edge created by earlier flake removal from the core. The striking platform is plain and not faceted. Flake LIA-187 has a natural dorsal surface, but shows an irregular retouch on the right lateral edge. The striking platform is an irregular natural surface.

Some of the smaller fragments are highly weathered due to the humic and acidic sedimentary environment, so their artificial origin is ambiguous. However, based on the occurrence of two unequivocal artefacts in juxtaposition, together with various flint fragments and chips, and the parallel presence of only a few other gravel-sized rocks, we infer a veritable occupational layer to exist in the half-bog > 6 m below the surface.

## 5 | DISCUSSION

### 5.1 | Landscape evolution model

#### 5.1.1 | Late Saalian

The rapid disintegration of the Late Saalian Warthe stage ice-sheets at around 135 ka produced large amounts of melt-out run-off and a progressively increasing availability of free water in the hydrological cycle (Lambeck et al., 2006). In contrast to quickly rising precipitation values, vegetation developed with a certain time lag (Helmens, 2014) and was rather sparse (Menke & Tynni, 1984), leaving the surfaces prone to sediment erosion and redeposition for some time. This was amplified by sustaining (discontinuous) permafrost that hampered infiltration in favour of overland flow (Rowland et al., 2010). In the central Öring hills, the landscape dynamically responded to this impulse with linear erosion, creating the first order dry valleys that cut through Warthe stage glacial deposits, testifying to valley formation after the Warthe glacial maximum (Merk, 1975; Figure 3; Method S1). Two first order alluvial fans, associated with this linear erosion can be identified at the transition of the southern Öring and the Salzwedel Palaolake basin (Figure 3b). The eastern fan shows deep incision oriented due east. This incision is recognized both as a slight depression in the modern topography (Figures 3c and S3) and in the sediment logs of the borehole transect, where the basal Saalian tills were eroded prior to the Eemian (Figure 4). We argue that this incision can only be explained by fluvial downcutting in the adjacent Elbe River valley, being the base level of our study area. Fluvial incision is reported for the Saalian-Eemian transition in the lower Elbe reaches (Averdieck, 1976; Ehlers, 1990; Grube et al., 1976) and for several other central European rivers, and thought to have been triggered by the spilling-over of ice-dammed lakes in the downstream areas (e.g., De Clercq et al., 2018; Winsemann et al., 2015). Downcutting in

**TABLE 2** Results of pIRIR<sub>290</sub> dating, including  $D_e$ -values, calculated ages, the used age model, overdispersion (OD) and the number of aliquots passing the rejection criteria

Lab.-ID (L-EVA)	$D_e$ (Gyr), $1\sigma$	Age (ka), $1\sigma$	Age model	OD (%)	Number of aliquots
2026	$264.4 \pm 36.4$	$108.4 \pm 17.0$	minimum age	$33.3 \pm 1.4$	17
2027	$295.2 \pm 19.8$	$104.6 \pm 10.5$	weighted mean	$26.6 \pm 0.8$	24

the Elbe valley would have lowered the local base level required for this incision within the alluvial fan, thus creating the shortest continuous drainage channel from the dry valley in the southern Öring to the Elbe valley by retrogressive erosion (Figures S2 and S3B). The channel passage between Öring and Lemgow that had previously formed as an Elsterian tunnel valley (Voss, 1981) would have been reactivated and overdeepened by that retrogressive (fluvial) erosion. By contrast, the western alluvial fan (Figure 3b) lacks signs of posterior erosion. Therefore, the local base level must have remained untouched during and after fan formation, which could have been caused by the longer distance to the Elbe River valley. To sum up, the studied sediment basin most likely is part of a c. 7 km long palaeovalley system that drained the southeast Öring towards the ice-marginal valley of the River Elbe (Figures 3b, S2 and S3). Based on its irregular shape and course and lacking Saalian tills at the drilling bases, possible alternative interpretations of the basin as a large Saalian kettle hole or tunnel valley are provisionally rejected (e.g., Behre & Lade, 1986; Turner, 2000).

### 5.1.2 | Saalian-Eemian transition to early Eemian (PZ E I and PZ E II)

Subsequently, the lower areas of the palaeovalley system, including the incised basin within the alluvial fan, partially filled up with water and accommodated an elongated fingerlake. The reason for the

topographic disconnection of the initial palaeovalley from the Elbe River valley is not yet clear, nor is the position of the blockage. We suggest that slope deposition might have obstructed the channel in the narrow passage between Öring and Lemgow. The presumed extent of the lake (size c. 1.3 km<sup>2</sup>), depicted in Figure 3(b) is based on our own data and information from the borehole database of Lower Saxony (<https://nibis.lbeg.de/cardomap3/>). At the bottom of this lake, 2 m of the first clayey and then slightly humic silty lacustrine deposits were accumulated (Figure 7a). Concomitantly, on the slope, a half-bog formed just above or even within the capillary fringe of the (ground) water table. This allows to approximate the upper and lower boundaries of the water body, that is a water depth of ~12 m for PZ E II (Figure 7a).

This pre-temperate phase at the onset of Eemian, as defined by Turner and West (1968), is characterized by an expansion of *Betula* (tree-birches) in pollen zone (PZ) E I in northern Germany. It was followed by a strong increase of *Pinus* (pine) dominating in the succeeding *Pinus-Betula* PZ E II (Menke & Tynni, 1984). In contrast to the previous Holsteinian interglacial, during this initial expansion of boreal forest, *Picea* was absent, and vegetation had not yet densely covered the immature soils. Due to the dynamic depositional and erosional processes at the onset of the Eemian in the study area, PZ E I and PZ E II are nearly missing in the transect, with the likely exceptions of samples 2 and 11 (Table 1; Figure 4). Likewise, both initial Eemian pollen zones were also missing in the

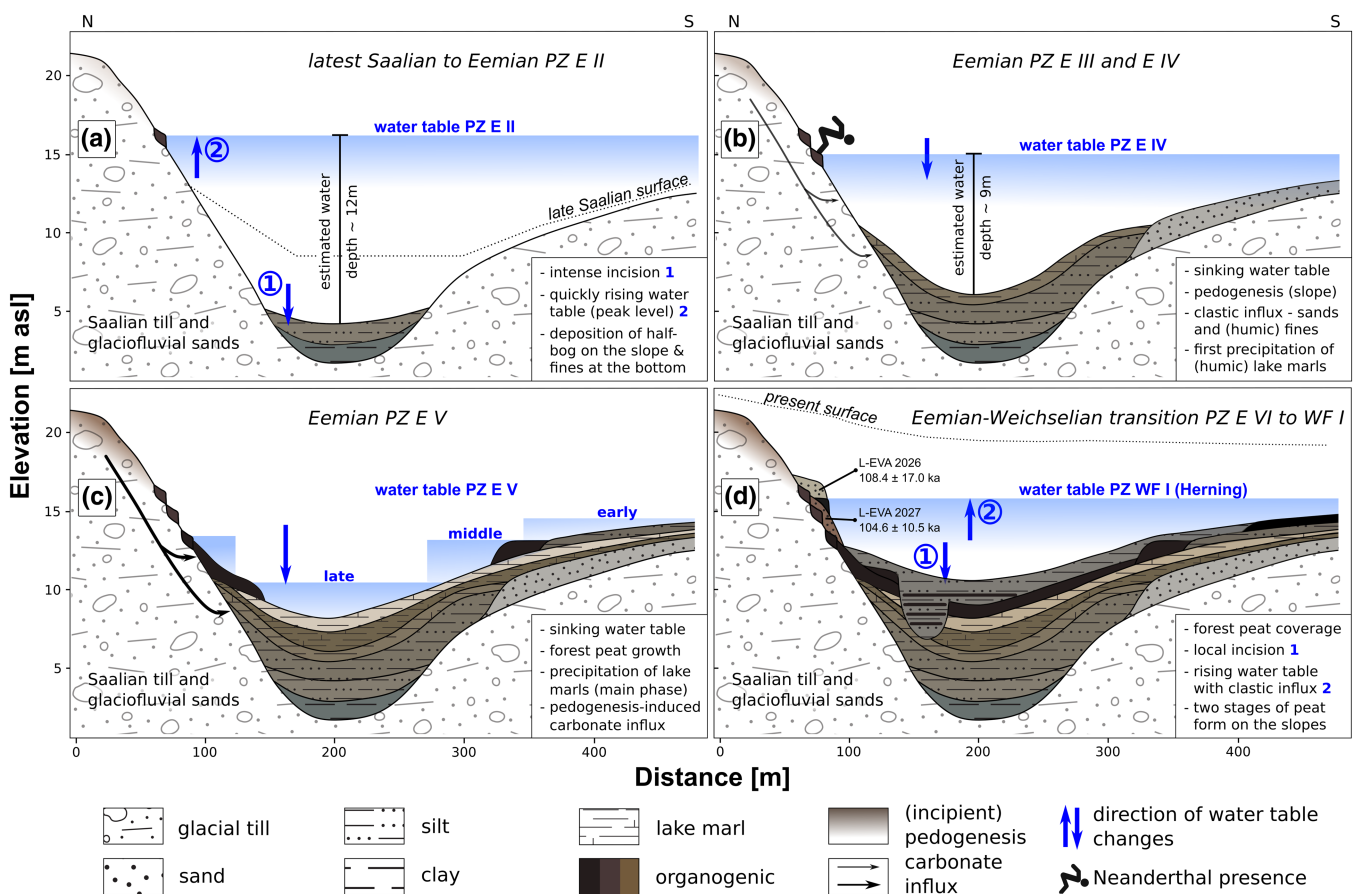


**FIGURE 7** Diachronic landscape evolution model of the study area that depicts the sedimentary and hydrological changes throughout the Eemian in four phases (following the classification of the Eemian cycle by Turner and West [1968]), PZ E I to E VII – Eemian pollen zones. PZ WF I – First Weichselian Stadial (PZ after Menke and Tynni [1984]) [Color figure can be viewed at [wileyonlinelibrary.com](http://wileyonlinelibrary.com)]

neighbouring palynological record formerly investigated by Veil et al. (1994).

### 5.1.3 | Early-temperate Eemian (PZ E III and E IV)

At the lake bottom, in continuation of the previous phase, more humic silts accumulated, grading upwards into (humic) lake marls. The latter testify to increasing landscape stability with pedogenesis in the exterior section, where decalcification and weathering of the Saalian tills must have led to carbonate-rich groundwater flow that caused the lake marl precipitation within the fingerlake (Figure 7b). This relationship has been described for various sites in northern Germany in previous studies (cf., Menke, 1992). On the steeper northern flank, half-bogs formed at a lower topographic elevation than during the previous phase. This documents a decreased water table compared with PZ E II. Together with the lake bottom sediments, this marginal facies allows for the estimation of the water depth to ~9 m (Figure 7b). Furthermore, a coeval waterside Palaeolithic encampment was inferred from artefact finds within the half-bog (Section 5.3). Also during this period, the deposition of calcareous coarse sand occurred on the shallow southern slope of the fingerlake, recorded in the cores Li-BPc and Li-BPd (Figures 4 and 7b). The presence of this coarser deposit seems to indicate higher-energy sedimentation compared with the dominant lacustrine sediments of that phase. Potentially, these sediments are of fluvial, colluvial or beach deposit character. Alternatively, the coarse sands might also have been mobilized by trampling animals in search for water, scarring the vegetation on their way (Butler et al., 2018).

The first deciduous taxa to expand were *Ulmus* (elm) and *Quercus* (oak). These rapidly became dominant and were characteristic of the *Pinus-Quercetum* mixtum (PZ E III) in the lower part of the early-temperate Eemian phase (Turner, 2000). Subsequently, a strong increase of *Corylus* (hazel) marks the transition towards pollen subzone E IVa (*Quercetum*-mixtum-*Corylus*). Pollen assemblages and preservation of a few samples hampered a clear division into subzones, resulting in a general assignment of those samples to PZ E IV (Table 1). The following pollen subzone E IVb, dominated by *Corylus* with *Tilia* (lime) and *Taxus* (yew), was however identified in some samples of the transect (Table 1). The Palaeolithic artefacts (core PD.030) derive from a late phase of PZ IVb transitioning into PZ V, when *Carpinus* (hornbeam) started to expand and *Corylus* declined (Table 1). The zonal vegetation, first rich in hazel, followed by lime, oak, elm

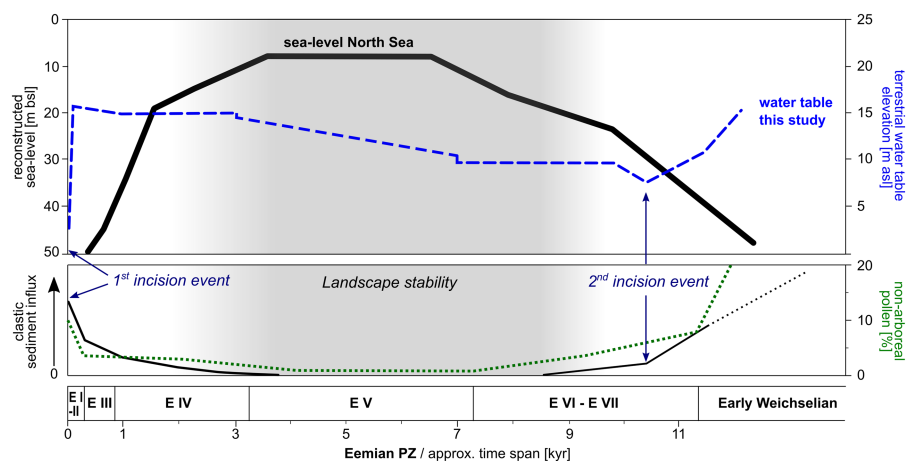
and yew, had apparently well colonized and stabilized the terrestrial soils in the vicinity of the site. Indicators for a temporally higher groundwater level and gleyic, swampy conditions are fern spores of the polypodi family (Polypodiaceae). Frequently, also *Typha latifolia*-type (cattail) and *Sparganium*-type (bur-reed) pollen occur. These wetland/aquatic plants usually border lakes, ponds or streams. The azonal vegetation of PZ E IV in Lichtenberg is furthermore characterized by minor, yet constant occurrences of Poaceae (grasses) and terrestrial herbs. These might point to a patchily-forested site, but could also be caused by trails created by trampling animals visiting open water sources.

### 5.1.4 | Late-temperate Eemian (PZ E V)

This phase was characterized by its distinct landscape stability and soil formation in the exterior, induced by a dense vegetation cover (Figures 7c and 8; Table 1). Apart from a thin veil of silt that was deposited at the southern flank during the early phase, no further clastic sedimentation can be recognized in the basin over some thousand years (cf., Müller, 1974). The intensive lake marl formation at the lake bottom and the southern slope distinctly points to a period of most pronounced decalcification and pedogenesis in the exterior, causing a high carbonate influx into the lake, and to generally warmer climatic conditions enabling carbonate precipitation during summer. Eemian decalcification and weathering of Saalian tills can exceed 4 m thickness in northern Germany, and was also observed in our cores PD.022 to PD.025 (Figures 4 and S4). Thus, soil formation is assumed to have been more intense than in comparable Holocene soils on Weichselian tills (Roeschmann et al., 1982; Stremme et al., 1982; Stephan, 2014). Lake marl deposition, as an indicator of intense soil formation during PZ E V has also been recognized in other central European and south Scandinavian sites, such as Lehringen (Thieme & Veil, 1985), Gröbern (Mania et al., 1990), Hollerup (Björck et al., 2000) and the Oderbruch basin in northeast Germany (Lüthgens et al., 2011).

During PZ E V, the water table gradually decreased at the study site. This is demonstrated by a half-bog on the steep south-facing slope, and two deviating lower levels of forest peat at the channel bottom and the shallow north-facing slope, respectively (Figure 7c). The upper peat at the basin bottom and the half-bog on the northern slope are situated at almost the same elevation. Since both require

**FIGURE 8** Upper panel – water table approximations of our study (blue) and Eemian North Sea-level progression (black) according to Zagwijn (1996) for comparison. Lower panel – semi-quantitative estimate of clastic influx and non-arboreal pollen through time at our study site. Horizontal scale for both panels – pollen zonation according to Menke and Tynni (1984), relative duration of the Eemian interglacial and the individual pollen zones after Müller (1974) [Color figure can be viewed at [wileyonlinelibrary.com](http://wileyonlinelibrary.com)]



similar moisture conditions for their formation and half-bogs are regarded as the incipient stage of peat development, the geomorphic position plausibly determined which types of organogenic sediments were formed (cf., Göttlich, 1965). Only flat and slightly sloping areas facilitated peat growth, whereas on steeper slopes, the shallow water zone was too narrow for peat formation and half-bogs prevailed instead. Estimating the water depth is challenging for this phase, because the marginal facies as a counterpart for the subaquatic sediments at the basin bottom is lacking for the better part of this phase. However, the water depth undoubtedly decreased, likely from about 7 m in the early to about 2 m at the later phase. During this late-temperate phase, the vegetation changed from *Corylus*, *Tilia*, *Quercetum-mixtum* to *Carpinus*-dominated forests. The more articulate predominance of AP over the NAP in the pollen records points to more densely vegetated areas in comparison to previous PZ E IV (Figure 8; Table 1). In combination with the sedimentological results, increasing values of *Alnus* (alder) indicate the expansion of local fen woodland. Furthermore, a decrease of Polypodiaceae and aquatic phanerogams versus an increase of taxa of the green algae genus *Pediastrum* might point to a change in the water trophic state (Turner et al., 2014).

### 5.1.5 | Late Eemian and Eemian/Weichselian transition

In PZ E VI, the water depth was further reduced until it was low enough for forest peat development at the bottom of the drying-out lake (Figure 7d). Hydrochemical conditions are assumed to have been rather acidic, as is implied by the non-calcareous forest peat in cores PD.029 and Li-BPa, enveloped by highly calcareous sediments above and underneath. Strong acidification during the later Eemian has also been reported by Roeschmann et al. (1982) and Menke (1992), who ascribed this effect to the decrease of thermophilous taxa and the establishment of conifer dominance in combination with carbonate-depleted substrates. In contrast to the nearby sequence in Veil et al. (1994), the deposits of the later PZ E VI and PZ E VII reflect changes in vegetation from the *Pinus-Picea-Abies*- to the *Pinus*-zone. This phase in our record is characterized by high percentages of reworked pollen, indicating the end of the long-lasting stability phase (between PZ E IV to E VI) and a resumption of higher geomorphic activity. Accordingly, this is supported by renewed erosion at the basin bottom, evident in core PD.032 and seismic data (Figures 4, 5 and 7d and Section 4.1). Similarly to the major first erosion during the Saalian-Eemian transition, we assume fluvial incision in the neighbouring Elbe River valley that retrogressively affected the lake basin by lowering the local base level. Incision during that time is known for many European rivers (Antoine et al., 2007; De Clercq et al., 2018; Gibbard & Lewin, 2002; Winsemann et al., 2015). In Lichtenberg, the subsequent deposition of several metres of humic silts indicates a progressively rising water table that fostered peat formation at a more elevated position on the shallow southern slope. Thus, a temporary stagnation in PZ E VII is inferred (Figure 7d). The following water level rise in the transitional period to the Hering Stadal (~MIS 5d) resulted in further siltation at the bottom of the restored fingerlake and in the aggradation of sandy slope deposits on the northern flank. Eventually, at high-stand conditions, a Hering-time sandy peat

developed and interfingers with these sands (PD.030). These deposits are bracketed by luminescence ages of  $105 \pm 10$  and  $108 \pm 17$  ka (Section 4.3, Figures 6a and 7d). This is in agreement with the end of the Eemian interglacial, as dated by Lüthgens et al. (2011) to  $108.9 \pm 7.8$  ka in northeast Germany. The presence of this peat points to a broader shallow-water zone on the northern flank compared to the early/mid-Eemian, when only half-bogs formed there. Unlike previously assumed by us (Section 4.1), peat growth during the Hering Stadal also means that organogenic deposits did not exclusively form during more temperate intervals. Instead, the climate throughout the Early Weichselian seems to have been warm enough to promote peat formation even during the Stadials, with the main limiting factor possibly being moisture rather than temperature at these latitudes. Similar suggestions have been made by Caspers et al. (2002) and Vandenberghe and van der Plicht (2016) for the MIS 3 in central Europe. The Hering-time sandy slope deposits on the northern flank, locally restricted to cores PD.026 and PD.030 (Figure 4, below pollen samples 1 and 3), tentatively represent an incipient stage of the formation of the second order alluvial fan (Figures 3c and S3).

## 5.2 | Synopsis of Eemian landscape dynamics

Three semi-quantitative proxies derived from our data give complementary information on the geomorphic activity and the hydrological development throughout the Eemian in the study area (Figure 8): Clastic sediment influx, the water table of the fingerlake (rather than its estimated depth) and the NAP. The latter have widely been used for a long time to approximate landscape openness in various studies (e.g., Faegri et al., 1989). Openness in turn, is known to be closely linked to the vulnerability of landscapes towards sediment erosion (Rohdenburg, 1970). Although the relationship between NAP and openness is complex and non-linear (e.g., Sugita et al., 1999), an NAP-based assessment of vegetation density can be reliable if additional parameters are consulted and relatively small surface areas are considered (cf., Favre et al., 2008).

In Lichtenberg, we observe a clear relationship between clastic sediment influx and NAP: Two phases of distinct geomorphic activity are indicated by higher values of both parameters. Surprisingly, even NAP amounts as low as c. 5% already correlate with considerable sediment input (Figure 8). These sediments were most likely provided by slope erosion from the shores of the fingerlake, or alternatively by deflation in its surroundings (cf., Schokker et al., 2004). The first activity phase already began in the late Saalian with the melt-out of the Warthe stage ice sheets and the dissection of the Öring by the first order dry valleys. It terminated not before Eemian PZ IV, roughly coinciding with the establishment of close deciduous woodlands (cf., Caspers et al., 2002). The second activity phase started in E PZ VI/VII and continued well into the Hering Stadal (Figure 8). Notably, both phases share common properties:

- i. They correspond to major climatic transitions at the beginning and end of the interglacial, when the sedimentary, hydrological and vegetational regimes adjusted to changing climatic conditions.

- ii. They broadly concur with local incision events, tentatively initiated by fluvial downcutting in the neighbouring Elbe River valley. Both incision events were followed by a rapid rise in lake level, possibly as a consequence of incomplete forests, leading to high effective precipitation and intensive surface run-off (cf., Behre et al., 2005; Börner et al., 2018; Fränzle, 1988; Kotaczek et al., 2016; Schokker et al., 2004; but see Mirosław-Grabowska, 2009 for late Eemian desiccating basins in Poland).
- iii. The vegetation during these phases is characterized by dominant boreal woodlands. These are nowadays known to be fire regimes and to be driven largely by disturbance and selective scarring of the plant cover (cf., de Groot et al., 2013), which fosters geomorphic activity.

A prolonged period of extensive landscape stability in between these two activity phases lasted from late PZ E IV to PZ E VI, equivalent to about 6000 years (Müller, 1974). Similar observations are known from the Roer Valley Graben, the Netherlands (Schokker et al., 2004). We detected no clastic sediment deposition during that time. Instead, widespread lake marls testify to densely vegetated, stable surfaces in the area, and dominating decalcification and pedogenesis on the Saalian substrates. This agrees with the NAP that reach their lowest average values of < 2% in this part of our record. Dense vegetation however, also induces high evapotranspiration rates, accompanied by dropping (ground)water levels (Helmens, 2014; Larsen et al., 2020). Accordingly, and despite an oceanic climate at that time (Kühl et al., 2007), the water table of the fingerlake was gradually dropping during the mid-Eemian. Yet, it was still high enough to allow peat and even lake marl deposition. In contrast, at many other study sites in central Europe, lacking sedimentary remains from PZ E IV and V indicate complete desiccation (e.g., Schokker et al., 2004, and references cited therein). In Lichtenberg, the groundwater levels surpassed the surface elevation, owing to the relatively large accommodation space, provided by the initial erosion of the palaeochannel that later hosted this fingerlake.

Contrary to our findings of a stable landscape, various studies described a mid-Eemian cold episode at different sites (e.g., Field et al., 1994; Helmens et al., 2015; Seidenkrantz et al., 1995). Such a climatic deterioration would have decreased the density of forest cover and thereby have allowed erosional and associated depositional processes. This assumption cannot be confirmed by the presented Lichtenberg record (cf., Cheddadi et al., 1998; Kühl et al., 2007; Kupryjanowicz et al., 2018).

### 5.3 | The middle Palaeolithic finds of Lichtenberg in the context of established Eemian occupations

The archaeological finds from late PZ E IV in core PD.030 define Lichtenberg as the northernmost Eemian Palaeolithic site narrowly ahead of Lehringen, Lower Saxony (Nielsen et al., 2015; Thieme & Veil, 1985). This spatial pattern may however be biased, as most Eemian occupations are former lake sites that are currently often buried below several metres of sediments. Therefore, most sites were primarily recovered during lignite mining in central Germany (see references to the sites mentioned later). A recent geographic analysis (Nielsen et al., 2019) has shown that Neanderthals could potentially

not have reached areas much further north, since the higher Eemian sea level compared with today disconnected Jutland and southern Scandinavia from northern Germany by a marine channel (Larsen et al., 2009). Furthermore, Weichselian glaciers have likely devastated possible evidence for occupation in (southern) Scandinavia.

A cluster of Eemian archaeological sites is known from central Germany (Figure 1): Repeated Neanderthal occupations in Neumark-Nord, Saxony-Anhalt in the central German dry area are documented from PZ E III to E IVb particularly during phases of a more open environment and higher lake-levels (Pop & Bakels, 2015; Strahl et al., 2010). The sites of Rabutz/ Saxony (Toepfer, 1958), Gröbern/ Saxony-Anhalt (Litt & Weber, 1988; Mania et al., 1990) and Grabschütz/Saxony (Weber, 1990) at the margin of this dry area show occupations during PZ E IV, the IVb/V-transition and PZ E VI. Similar semi-open environments can also be expected for this region. In comparison, Lehringen (occupation in PZ E IVb) (Thieme & Veil, 1985) and Lichtenberg (PZ E IVb/V transition) are situated in northern Germany, and a more oceanic climate with a denser vegetation cover can be assumed for that time (Menke, 1992; Menke & Tynni, 1984; this study).

Interestingly, the known archaeological record of Eemian sites seems to omit (i) the main part of the Eemian temperate zone (PZ E V), and (ii) the beginning and termination of the Eemian interglacial. Pollen zone E V coincides with a distinct landscape stability (Section 5.2, Figures 7c and 8). Therefore, on the one hand, the availability of lithic raw material for tool production was rather limited, and on the other hand, sedimentation processes that could have embedded artefacts hardly existed. Furthermore, low groundwater tables during PZ E V led to the desiccation of small lake basins (see Section 5.2), reducing the attraction of otherwise potential lake occupational sites. As for the shortage of archaeological sites from the early and late Eemian, potential evidence might have been destroyed or corrupted by sediment redeposition that we reconstructed for these times. Hence, landscape dynamics could well be one explanatory factor for the lack of registered sites in certain phases of the Eemian. Based on the information presented earlier, human occupation of lakeshores in northern and central Germany seemed to be quite common during PZ E III to IV/V. Therefore, artefact finds within the corresponding sediments in Lichtenberg match the currently expected Eemian Neanderthal settlement pattern.

## 6 | CONCLUSIONS

This geomorphological study was carried out at a palaeolake margin on the European Plain in northern Germany, where records of landscape activity and stability beyond coastal areas and river valleys are still largely missing. Relative (biostratigraphic) chronological control of the drilled sediments was obtained by taking bulk samples for pollen analysis distributed over the whole drilling transect, instead of single core sequences. This cost and time efficient approach granted us the required spatial resolution for robust inferences about the local Eemian landscape evolution. Within this context, the inevitably lower temporal resolution of the bulk pollen samples was no major obstruction.

Our results allow to understand the interactions of sediment deposition, hydrology and vegetation density during the Eemian

interglacial in this so far largely understudied area: Two phases of geomorphic activity occurred during main climatic shifts before the onset and towards the end of the Eemian. Intensive incision during the first active phase can chronologically be restricted to the late Saalian transition towards the earliest Eemian. Incision was triggered by rapidly changing climatic conditions and a sparse vegetation cover, and was amplified by a lowered local base level due to downcutting of the River Elbe in the adjacent ice-marginal valley. The resulting deep palaeovalley system in the hinterland of the Elbe valley soon accommodated a fingerlake, whose clastic sediment infilling waned during the pre-temperate Eemian (PZ E III/IV after Menke and Tynni [1984]). Contemporaneously, the water table of the fingerlake gradually sank on account of densely vegetated slopes dominated by deciduous woodlands. These stable conditions allowed soil formation, leading to decalcification on the slopes and resulting carbonate influx into the fingerlake where the carbonate precipitated as lake marl deposits. Mid-Eemian landscape stability lasted for c. 6000 years (esp. PZ E V), while the lake successively turned into a swampy depression without drying out completely. Geomorphic activity resumed during the late, post-temperate Eemian (PZ E VI/VII), when incision into the fingerlake deposits implies a renewed fluvial downcutting of the Elbe River and a drop of local base levels. Subsequently, a quickly rising water table refilled the fingerlake and was associated with increasing clastic sediment influx into the lake basin. This second phase of geomorphic activity continued even after the end of the Eemian in the following Herring Stadial. Despite this being a case study, we assume that these activity and stability phases may also apply to comparable landscape segments during this time (cf., Fränze, 1988; Garleff & Leontaris, 1971; Schokker et al., 2004).

Future studies will complement our findings with a multi-proxy and high-resolution analysis of core Li-BPa in the centre of the lake basin (Figure 4), allowing for more detailed reconstructions of the local palaeoenvironments. Furthermore, deciphering the sedimentary history of the Elbe River is part of future endeavours in order to better understand the connection of fluvial behaviour and the geomorphic phases in the hinterland.

Mid-Eemian Neanderthal occupation was observed on the former fingerlake shoreline during a time of marginal geomorphic activity and not yet entirely closed woodlands (PZ E IVb/V). This northernmost Eemian Neanderthal presence on the European Plain is a valuable data point to reconstruct the poorly understood human-environment relationship during that time (see references earlier, cf. Nicholson, 2017). Since the overall archaeological record is still very sparse and strongly biased, additional sites need to be discovered and investigated before Eemian occupation patterns can profoundly be reconstructed and interpreted.

## ACKNOWLEDGEMENTS

The authors thank the State Office for Mining, Energy and Geology of Lower-Saxony (LBEG) for use of their drilling rig, and Robert Broschinski and Thomas Jelinski for operating the machine. The authors also thank Jan Bergmann-Barrocas and Jan Bayerle who carried out the seismic survey. The authors owe their gratitude to families Dreier, Kusserow and Kohrs-Lichte for granting access to their land and to Nicolas Bourgon for supporting fieldwork and improving the manuscript. The authors thank Steffi Hesse and Victoria Krippner, who kindly conducted luminescence sample

preparation at the MPI EVA. The authors thankfully acknowledge the work done by the ESPL editors and two anonymous reviewers who helped to improve the manuscript. M.H. thanks Jean-Jacques Hublin and the Max Planck society (Max-Planck-Gesellschaft) for funding this study as part of his PhD.

## CONFLICT OF INTEREST

The authors declare that they have no known competing financial interests or personal relationships that could have appeared to influence the work reported in this article.


## DATA AVAILABILITY STATEMENT

The data that support the findings of this study are available from the corresponding authors upon reasonable request.

## ORCID

Michael Hein  <https://orcid.org/0000-0002-5500-4020>

David Colin Tanner  <https://orcid.org/0000-0002-9488-8631>

Hans von Suchodoletz  <https://orcid.org/0000-0002-4366-9383>

## REFERENCES

- Antoine, P., Coutard, S., Guerin, G., Deschodt, L., Goval, E., Loch, J.-L. & Paris, C. (2016) Upper Pleistocene loess-palaeosol records from northern France in the European context: Environmental background and dating of the Middle Palaeolithic. *Quaternary International*, 411, 4–24. Available from: <https://doi.org/10.1016/j.quaint.2015.11.036>
- Antoine, P., Limondin Lozouet, N., Chaussé, C., Lautridou, J.-P., Pestre, J.-F., Auguste, P. et al. (2007) Pleistocene fluvial terraces from northern France (Seine, Yonne, Somme): Synthesis, and new results from interglacial deposits. *Quaternary Science Reviews*, 26, 2701–2723. Available from: <https://doi.org/10.1016/j.quascirev.2006.01.036>
- Averdieck, F. R. (1976). Palynologische Untersuchungen zur Altersbestimmung und Vegetationsgeschichte des Alstertales. Mitt. Geol.-Paläont. Inst. Univ. Hamburg. Sonderband Alster: 81–89.
- Behre, K.-E., Hölzer, A. & Lemdahl, G. (2005) Botanical macro-remains and insects from the Eemian and Weichselian site of Oerel (northwest Germany) and their evidence for the history of climate. *Vegetation History and Archaeobotany*, 14, 31–53. Available from: <https://doi.org/10.1007/s00334-005-0059-x>
- Behre, K.-E. & Lade, U. (1986) Eine Folge von Eem und 4 Weichsel-Interstadialen in Oerel/Niedersachsen und ihr Vegetationsablauf. *E&G Quaternary Science Journal*, 36, 11–36. Available from: <https://doi.org/10.3285/eg.36.1.02>
- Beug, H.-J. (2004) Leitfaden der Pollenbestimmung für Mitteleuropa und angrenzende Gebiete. *Germania*, 87, 542.
- Björck, S., Noe-Nygaard, N., Wolin, J., Houmark-Nielsen, M., Jørgen Hansen, H. & Snowball, I. (2000) Eemian Lake development, hydrology and climate: a multi-stratigraphic study of the Hollerup site in Denmark. *Quaternary Science Reviews*, 19, 509–536. Available from: [https://doi.org/10.1016/S0277-3791\(99\)00025-6](https://doi.org/10.1016/S0277-3791(99)00025-6)
- Boden, A.-H.-A. (2005) Bodenkundliche Kartieranleitung. Bundesanstalt für Geowissenschaften und Rohstoffe. In: Diensten, G. (Ed.) *Zusammenarbeit mit den Staatlichen*, 5th edition. Hannover: Schweizerbart Science Publishers, pp. 141–147.
- Börner, A., Hrynowiecka, A., Stachowicz-Rybka, R., Niska, M., Moskal-del Hoyo, M., Kuznetsov, V. et al. (2018) Palaeoecological investigations and 230Th/U dating of the Eemian interglacial peat sequence from Neubrandenburg-Hinterste Mühle (Mecklenburg-Western Pomerania, NE Germany). *Quaternary International*, 467, 62–78. Available from: <https://doi.org/10.1016/j.quaint.2017.04.003>
- Brandes, C., Plenefisch, T., Tanner, D.C., Gesterma, N. & Steffen, H. (2019) Evaluation of deep crustal earthquakes in northern Germany – possible tectonic causes. *Terra Nova*, 31, 83–93. Available from: <https://doi.org/10.1111/ter.12372>

- Brauer, A., Allen, J.R.M., Mingram, J., Dulski, P., Wulf, S. & Huntley, B. (2007) Evidence for last interglacial chronology and environmental change from southern Europe. *PNAS*, 104, 450–455. Available from: <https://doi.org/10.1073/pnas.0603321104>
- Busschers, F.S., Kasse, C., van Balen, R.T., Vandenberghe, J., Cohen, K.M., Weerts, H.J.T. et al. (2007) Late Pleistocene evolution of the Rhine-Meuse system in the southern North Sea basin: Imprints of climate change, sea-level oscillation and glacio-isostasy. *Quaternary Science Reviews*, 26, 3216–3248. Available from: <https://doi.org/10.1016/j.quascirev.2007.07.013>
- Butler, D.R., Anzah, F., Goff, P.D. & Villa, J. (2018) Zoogeomorphology and resilience theory. *Geomorphology*, 305, 154–162. Available from: <https://doi.org/10.1016/j.geomorph.2017.08.036>
- Caspers, G., Merkt, J., Müller, H. & Freund, H. (2002) The Eemian Interglaciation in northwestern Germany. *Quaternary Research*, 58, 49–52. Available from: <https://doi.org/10.1006/qres.2002.2341>
- Cheddadi, R., Mamakowa, K., Guiot, J., de Beaulieu, J.-L., Reille, M., Andrieu, V. et al. (1998) Was the climate of the Eemian stable? A quantitative climate reconstruction from seven European pollen records. *Palaeogeography, Palaeoclimatology, Palaeoecology*, 143, 73–85. Available from: [https://doi.org/10.1016/S0031-0182\(98\)00067-4](https://doi.org/10.1016/S0031-0182(98)00067-4)
- De Clercq, M., Missiaen, T., Wallinga, J., Zurita Hurtado, O., Versendaal, A., Mathys, M. & De Batist, M. (2018) A well-preserved Eemian incised-valley fill in the southern North Sea Basin, Belgian Continental Shelf – Coastal Plain: Implications for northwest European landscape evolution. *Earth Surface Processes and Landforms*, 43, 1913–1942. Available from: <https://doi.org/10.1002/esp.4365>
- de Groot, W.J., Cantin, A.S., Flannigan, M.D., Soja, A.J., Gowman, L.M. & Newbery, A. (2013) A comparison of Canadian and Russian boreal forest fire regimes. *Forest Ecology and Management*, 294, 23–34. Available from: <https://doi.org/10.1016/j.foreco.2012.07.033>
- Duphorn, K., Grube, F., Meyer, K.-D., Streif, H. & Vinken, R. (1973) A. Area of Scandinavian Glaciation: 1. Pleistocene and Holocene. *E&G Quaternary Science Journal*, 23/24, 222–250. Available from: <https://doi.org/10.3285/eg.23-24.1.19>
- Ehlers, J. (1990) Untersuchungen zur Morphodynamik der Vereisungen Norddeutschlands unter Berücksichtigung benachbarter Gebiete. *Bremer Beiträge Zur Geographie Und Raumplanung*, 19, 166.
- Ehlers, J. (2020) *Das Eiszeitalter*. Berlin: Springer Available from: <http://link.springer.com/10.1007/978-3-662-60582-0>
- Ehlers, J. & Gibbard, P.L. (2004) Quaternary glaciations extent and chronology - Part I: Europe. *Developments in Quaternary Sciences*. Available from: [https://doi.org/10.1016/S1571-0866\(04\)80056-3](https://doi.org/10.1016/S1571-0866(04)80056-3)
- Ehlers, J., Grube, A., Stephan, H.J. & Wansa, S. (2011) Pleistocene glaciations of north Germany – new results. *Developments in Quaternary Science*, 15, 149–162. Available from: <https://doi.org/10.1016/B978-0-444-53447-7.00013-1>
- Ehlers, J., Meyer, K.-D. & Stephan, H.-J. (1984) The pre-weichselian glaciations of north-west Europe. *Quaternary Science Reviews*, 3, 1–40. Available from: [https://doi.org/10.1016/0277-3791\(84\)90003-9](https://doi.org/10.1016/0277-3791(84)90003-9)
- Fægri, K., Iversen, J., Kaland, P.E. & Krzywinski, K. (1989) *Textbook of pollen analysis*, 4th edition. Chichester: John Wiley & Sons.
- Favre, E., Escarguel, G., Suc, J.-P., Vidal, G. & Thévenod, L. (2008) A contribution to deciphering the meaning of AP/NAP with respect to vegetation cover. *Review of Palaeobotany and Palynology*, 148, 13–35. Available from: <https://doi.org/10.1016/j.revpalbo.2007.08.003>
- Field, M.H., Huntley, B. & Müller, H. (1994) Eemian climate fluctuations observed in a European pollen record. *Nature*, 371, 779–783. Available from: <https://doi.org/10.1038/371779a0>
- Fränzle, O. (1988) Glaziäre, periglaziäre und marine Reliefentwicklung im nördlichen Schleswig-Holstein. *Schriften des Naturwissenschaftlichen Vereins für Schleswig-Holstein*, 58, 1–30.
- Garleff, K. & Leontaris, S.N. (1971) Jungquartäre Taleintiefung und Flächenbildung am Wilseder Berg (Lüneburger Heide). *E&G Quaternary Science Journal*, 22, 148–155. Available from: <https://doi.org/10.3285/eg.22.1.11>
- Gibbard, P. & Lewin, J. (2002) Climate and related controls on interglacial fluvial sedimentation in lowland Britain. *Sedimentary Geology*, 151, 187–210. Available from: [https://doi.org/10.1016/S0037-0738\(01\)00253-6](https://doi.org/10.1016/S0037-0738(01)00253-6)
- Göttlich, K. (1965) Ergebnisse und Ziele bodenkundlicher Studien in Moor und Anmoor. Dargelegt an hypopedologischen Untersuchungen in Südwestdeutschland. *Arbeiten der Landwirtschaftlichen Hochschule Hohenheim*, 33, 121.
- Grimm, E. C. (1990). TILIA, TILIAGRAPH and TILIAVIEW. PC spreadsheet and graphics software for pollen data. Available from: [www.geo.arizona.edu/palynology/geos581/tiliaview.html](http://www.geo.arizona.edu/palynology/geos581/tiliaview.html)
- Grube, F., Vladi, F. & Vollmer, T. (1976). Erdgeschichtliche Entwicklung des unteren Alstertales. Mitt. Geol.-Paläont. Inst. Univ. Hamburg. Sonderband Alster: 43–56.
- Haesaerts, P. & Mestdagh, H. (2000) Pedosedimentary evolution of the last interglacial and early glacial sequence in the European loess belt from Belgium to central Russia. *Netherlands Journal of Geosciences*, 79, 313–324. Available from: <https://doi.org/10.1017/S001677460002179X>
- Head, M.J., Seidenkrantz, M.-S., Janczyk-Kopikowa, Z., Marks, L. & Gibbard, P.L. (2005) Last Interglacial (Eemian) hydrographic conditions in the southeastern Baltic Sea, NE Europe, based on dinoflagellate cysts. *Quaternary International*, 130, 3–30. Available from: <https://doi.org/10.1016/j.quaint.2004.04.027>
- Hein, M., Weiss, M., Otcherednoy, A. & Lauer, T. (2020) Luminescence chronology of the key-Middle Paleolithic site Khotylevo I (western Russia) – implications for the timing of occupation, site formation and landscape evolution. *Quaternary Science Advances*, 2, 100008. Available from: <https://doi.org/10.1016/j.qsa.2020.100008>
- Helmens, K.F. (2014) The last interglacial-glacial cycle (MIS 5–2) re-examined based on long proxy records from central and northern Europe. *Quaternary Science Reviews*, 86, 115–143. Available from: <https://doi.org/10.1016/j.quascirev.2013.12.012>
- Helmens, K.F., Salonen, J.S., Pliikk, A., Engels, S., Väliiranta, M., Kylander, M. et al. (2015) Major cooling intersecting peak Eemian interglacial warmth in northern Europe. *Quaternary Science Reviews*, 122, 293–299. Available from: <https://doi.org/10.1016/j.quascirev.2015.05.018>
- Höfle, H.-C., Merkt, J. & Müller, H. (1985) Die Ausbreitung des Eem-Meeres in Nordwestdeutschland. *E&G Quaternary Science Journal*, 35, 49–60. Available from: <https://doi.org/10.3285/eg.35.1.09>
- Högberg, M.N., Högberg, P. & Myrold, D.D. (2006) Is microbial community composition in boreal forest soils determined by pH, C-to-N ratio, the trees, or all three? *Oecologia*, 150, 590–601. Available from: <https://doi.org/10.1007/s00442-006-0562-5>
- Illies, H. (1954) Entstehung und eiszeitliche Geschichte der unteren Elbe. *Mitteilungen aus dem Geologischen Staatsinstitut in Hamburg*, 23, 42–49.
- Kolaczek, P., Niska, M., Mirosław-Grabowska, J. & Gałka, M. (2016) Periodic lake-peatland shifts under the Eemian and Early Weichselian climate changes in central Europe on the basis of multi-proxy studies. *Palaeogeography, Palaeoclimatology, Palaeoecology*, 461, 29–43. Available from: <https://doi.org/10.1016/j.palaeo.2016.08.002>
- Krawczyk, C.M., Polom, U., Trabs, S. & Dahm, T. (2012) Sinkholes in the city of Hamburg—new urban shear-wave reflection seismic system enables high-resolution imaging of subsurface structures. *Journal of Applied Geophysics*, 78, 133–143. Available from: <https://doi.org/10.1016/j.jappgeo.2011.02.003>
- Kühl, N., Litt, T., Schölzel, C. & Hense, A. (2007) Eemian and Early Weichselian temperature and precipitation variability in northern Germany. *Quaternary Science Reviews*, 26, 3311–3317. Available from: <https://doi.org/10.1016/j.quascirev.2007.10.004>
- Kupryjanowicz, M., Fiłoc, M. & Kwiatkowski, W. (2018) Was there an abrupt cold climatic event in the middle Eemian? Pollen record from a palaeolake at the Hieronimowo site, NE Poland. *Quaternary International*, 467, 96–106. Available from: <https://doi.org/10.1016/j.quaint.2017.04.027>
- Lambeck, K., Purcell, A., Funder, S., Kjaer, K.H., Larsen, E. & Møller, P. (2006) Constraints on the Late Saalian to early Middle Weichselian ice sheet of Eurasia from field data and rebound modelling. *Boreas*, 35, 539–575. Available from: <https://doi.org/10.1080/03009480600781875>



- Lang, J., Lauer, T. & Winsemann, J. (2018) New age constraints for the Saalian glaciation in northern central Europe: Implications for the extent of ice sheets and related proglacial lake systems. *Quaternary Science Reviews*, 180, 240–259. Available from: <https://doi.org/10.1016/j.quascirev.2017.11.029>
- Larsen, A., Nardin, W., Lageweg, W.I. & Bätz, N. (2020) Biogeomorphology, quo vadis? On processes, time, and space in biogeomorphology. *Earth Surface Processes and Landforms*, 46(1), 12–23. Available from: <https://doi.org/10.1002/esp.5016>
- Larsen, N.K., Knudsen, K.L., Krohn, C.F., Kronborg, C., Murray, A.S. & Nielsen, O.B. (2009) Late Quaternary ice sheet, lake and sea history of southwest Scandinavia – a synthesis. *Boreas*, 38(4), 732–761. Available from: <https://doi.org/10.1111/j.1502-3885.2009.00101.x>
- Lisiecki, L.E. & Raymo, M.E. (2005) A Plio-Pleistocene stack of 57 globally distributed benthic  $\delta^{18}O$  records. *Paleoceanography*, 20(1), PA1003. Available from: <https://doi.org/10.1029/2004PA001071>
- Litt, T. & Weber, T. (1988) Ein eemzeitlicher Waldelefantenschlachtplatz von Gröbern, Krs. Gräfenhainichen. *Ausgrabungen und Funde*, 33, 181–187.
- Lüthgens, C., Böse, M., Lauer, T., Krbetschek, M., Strahl, J. & Wenske, D. (2011) Timing of the last interglacial in Northern Europe derived from Optically Stimulated Luminescence (OSL) dating of a terrestrial Saalian–Eemian–Weichselian sedimentary sequence in NE-Germany. *Quaternary International*, 241, 79–96. Available from: <https://doi.org/10.1016/j.quaint.2010.06.026>
- Lüttig, G. & Meyer, K. D. (1974). Geological history of the River Elbe, mainly of its lower course. *Annales de la Société géologique de Belgique. L'évolution quaternaire des bassins fluviaux de la Mer du Nord méridionale: 1–19.*
- Mania, D., Thomae, M., Litt, T. & Weber, T. (1990) Neumark - Gröbern. Beiträge zur Jagd des mittelpaläolithischen Menschen. *Veröffentlichungen des Landesmuseums für Vorgeschichte Halle*, 43, 321.
- Marks, L., Gałazka, D., Krzywińska, J., Nita, M., Stachowicz-Rybka, R., Witkowski, A. et al. (2014) Marine transgressions during Eemian in northern Poland: A high resolution record from the type section at Cierpięta. *Quaternary International*, 328–329, 45–59. Available from: <https://doi.org/10.1016/j.quaint.2013.12.007>
- Matoshko, A. V. (2011). Limits of the Pleistocene Glaciations in the Ukraine. In 405–418. Available from: <https://linkinghub.elsevier.com/retrieve/pii/B9780444534477000313>
- Meier-Uhlherr, R., Schulz, C. & Luthardt, V. (2015) *Steckbriefe Moorsubstrate*, 2nd. edition. Berlin: HNE Eberswalde.
- Menke, B. (1992) Eeminterglaziale und nacheiszeitliche Wälder in Schleswig-Holstein. *GLASH*, 1, 29–101.
- Menke, B. & Tynni, R. (1984) Das Eeminterglazial und das Weichselfrühglazial von Rederstell/Dithmarschen und ihre Bedeutung für die mitteleuropäische Jungpleistozän-Gliederung. *Geologisches Jahrbuch A*, 76, 1–120.
- Merk, J. (1975) *Geologische Karte von Niedersachsen 1:25000, Blatt 3033 Woltersdorf*. Energie und Geologie (LBEG) Hannover: Landesamt für Bergbau.
- Meyer, K.D. (1983) Zur Anlage der Urstromtäler in Niedersachsen. *Zeitschrift für Geomorphologie*, 27, 147–160.
- Miettinen, A., Head, M.J. & Knudsen, K.L. (2014) Eemian sea-level highstand in the eastern Baltic Sea linked to long-duration White Sea connection. *Quaternary Science Reviews*, 86, 158–174. Available from: <https://doi.org/10.1016/j.quascirev.2013.12.009>
- Miroslaw-Grabowska, J. (2009) Evolution of palaeolake environment in Poland during the Eemian interglacial based on oxygen and carbon isotope data from lacustrine carbonates. *Quaternary International*, 207, 145–156. Available from: <https://doi.org/10.1016/j.quaint.2009.05.004>
- Moore, P.D., Webb, J.A. & Collison, M.E. (1991) *Pollen Analysis*. Oxford: Blackwell Scientific Publications.
- Müller, H. (1974) Pollenanalytische Untersuchungen und Jahresschichtenzählungen an der eemzeitlichen Kieselgur von Bisingen/Luhe. *Geologisches Jahrbuch*, A21, 149–169.
- Nelson, M., Rittenour, T. & Cornachione, H. (2019) Sampling Methods for Luminescence Dating of Subsurface Deposits from Cores. *Methods and Protocols*, 2, 88. Available from: <https://doi.org/10.3390/mps2040088>
- Nicholson, C.M. (2017) Eemian paleoclimate zones and Neanderthal landscape-use: A GIS model of settlement patterning during the last interglacial. *Quaternary International*, 438, 144–157. Available from: <https://doi.org/10.1016/j.quaint.2017.04.023>
- Nielsen, T.K., Benito, B.M., Svenning, J.C., Sandel, B., McKerracher, L., Riede, F. & Kjaergaard, P.C. (2015) Investigating Neanderthal dispersal above 55°N in Europe during the Last Interglacial Complex. *Quaternary International*, 431, 88–103. Available from: <https://doi.org/10.1016/j.quaint.2015.10.039>
- Nielsen, T.K., Kristiansen, S.M. & Riede, F. (2019) Neanderthals at the frontier? Geological potential of southwestern South Scandinavia as archive of Pleistocene human occupation. *Quaternary Science Reviews*, 221, 105870. Available from: <https://doi.org/10.1016/j.quascirev.2019.105870>
- Peeters, J., Busschers, F.S. & Stouthamer, E. (2015) Fluvial evolution of the Rhine during the last interglacial-glacial cycle in the southern North Sea basin: A review and look forward. *Quaternary International*, 357, 176–188. Available from: <https://doi.org/10.1016/j.quaint.2014.03.024>
- Pop, E. & Bakels, C. (2015) Semi-open environmental conditions during phases of hominin occupation at the Eemian interglacial basin site Neumark-Nord 2 and its wider environment. *Quaternary Science Reviews*, 117, 72–81. Available from: <https://doi.org/10.1016/j.quascirev.2015.03.020>
- Reicherter, K., Kaiser, A. & Stackebrandt, W. (2005) The post-glacial landscape evolution of the North German Basin: Morphology, neotectonics and crustal deformation. *International Journal of Earth Sciences*, 94, 1083–1093. Available from: <https://doi.org/10.1007/s00531-005-0007-0>
- Roeschmann, G., Ehlers, J., Meyer, B., Rohdenburg, H. & Benzler, J.-H. (1982) Paläoböden in Niedersachsen, Bremen und Hamburg. *Geologisches Jahrbuch, Reihe F*, 14, 255–309.
- Rohdenburg, H. (1970) Morphodynamische Aktivitäts- und Stabilitätszeiten statt Pluvial- und Interpluvialzeiten. *E&G Quaternary Science Journal*, 21, 81–96. Available from: <https://doi.org/10.3285/eg.21.1.07>
- Rother, H., Lorenz, S., Börner, A., Kenzler, M., Siermann, N., Fülling, A. et al. (2019) The terrestrial Eemian to late Weichselian sediment record at Beckentin (NE-Germany): First results from lithostratigraphic, palynological and geochronological analyses. *Quaternary International*, 501, 90–108. Available from: <https://doi.org/10.1016/j.quaint.2017.08.009>
- Rowland, J.C., Jones, C.E., Altmann, G., Bryan, R., Crosby, B.T., Hinzman, L. D. et al. (2010) Arctic landscapes in transition: Responses to thawing permafrost. *Eos, Transactions American Geophysical Union*, 91(26), 229–230. Available from: <https://doi.org/10.1029/2010EO260001>
- Schokker, J., Cleveringa, P. & Murray, A.S. (2004) Palaeoenvironmental reconstruction and OSL dating of terrestrial Eemian deposits in the southeastern Netherlands. *Journal of Quaternary Science*, 19, 193–202. Available from: <https://doi.org/10.1002/jqs.808>
- Seidenkrantz, M.-S., Kristensen, P. & Knudsen, K.L. (1995) Marine evidence for climatic instability during the last interglacial in shelf records from northwest Europe. *Journal of Quaternary Science*, 10, 77–82. Available from: <https://doi.org/10.1002/jqs.3390100108>
- Shackleton, N.J., Chapman, M., Sánchez-Goni, M.F., Paillet, D. & Lancelot, Y. (2002) The Classic Marine Isotope Substage 5e. *Quaternary Research*, 58, 14–16. Available from: <https://doi.org/10.1006/qres.2001.2312>
- Sier, M.J., Peeters, J., Dekkers, M.J., Parés, J.M., Chang, L., Busschers, F.S. et al. (2015) The Blake Event recorded near the Eemian type locality – a diachronic onset of the Eemian in Europe. *Quaternary Geochronology*, 28, 12–28. Available from: <https://doi.org/10.1016/j.quageo.2015.03.003>
- Stephan, H.-J. (2014) Climato-stratigraphic subdivision of the Pleistocene in Schleswig-Holstein, Germany and adjoining areas: Status and problems. *E&G Quaternary Science Journal*, 63, 3–18. Available from: <https://doi.org/10.3285/eg.63.1.01>
- Strahl, J., Krbetschek, M.R., Luckert, J., Machalet, B., Meng, S., Oches, E.A. et al. (2010) Geologie, Paläontologie und Geochronologie des

- Eem-Beckens Neumark-Nord 2 und Vergleich mit dem Becken Neumark-Nord 1 (Geiseltal, Sachsen-Anhalt). *Eiszeitalter und Gegenwart (Quaternary Science Journal)*, 59, 120–167. Available from: <https://doi.org/10.3285/eg.59.1-2.09>
- Streif, H. (2004) Sedimentary record of Pleistocene and Holocene marine inundations along the North Sea coast of Lower Saxony, Germany. *Quaternary International*, 112, 3–28. Available from: [https://doi.org/10.1016/S1040-6182\(03\)00062-4](https://doi.org/10.1016/S1040-6182(03)00062-4)
- Stremme, H., Felix-Henningsen, P., Weinhold, H. & Christensen, S. (1982) Paläoböden in Schleswig-Holstein. *Geologisches Jahrbuch, Reihe F*, 14, 311–361.
- Sugita, S., Gaillard, M.-J. & Broström, A. (1999) Landscape openness and pollen records: A simulation approach. *The Holocene*, 9, 409–421. Available from: <https://doi.org/10.1191/095968399666429937>
- Thiel, C., Buylaert, J.P., Murray, A., Terhorst, B., Hofer, I., Tsukamoto, S. & Frechen, M. (2011) Luminescence dating of the Stratzing loess profile (Austria) – testing the potential of an elevated temperature post-IR IRSL protocol. *Quaternary International*, 234(1–2), 23–31. Available from: <https://doi.org/10.1016/j.quaint.2010.05.018>
- Thieme, H. & Veil, S. (1985) Neue Untersuchungen zum eemzeitlichen Elefanten-Jagdplatz Lehringen, Ldkr. *Die Kunde, Neue Folge (N.F.)*, 36, 11–58.
- Toepfer, V. (1958) Steingeräte und Palökologie der mittel- paläolithischen Fundstelle Rabutz bei Halle. *Jahresschrift für Mitteldeutsche Vorgeschichte*, 41/42, 140–179.
- Turner, C. (2000) The Eemian interglacial in the North European plain and adjacent areas. *Netherlands Journal of Geosciences*, 79, 217–231. Available from: <https://doi.org/10.1017/S0016774600023660>
- Turner, C. (2002) Formal status and vegetational development of the Eemian interglacial in northwestern and southern Europe. *Quaternary Research*, 58, 41–44. Available from: <https://doi.org/10.1006/qres.2002.2365>
- Turner, C. & West, R.G. (1968) The subdivision and zonation of interglacial periods. *E&G Quaternary Science Journal*, 19, 93–101. Available from: <https://doi.org/10.3285/eg.19.1.06>
- Turner, F., Tolktsdorf, J.F., Viehberg, F., Schwab, A., Kaiser, K., Bittmann, F. et al. (2013) Lateglacial/early Holocene fluvial reactions of the Jeetzel River (Elbe valley, northern Germany) to abrupt climatic and environmental changes. *Quaternary Science Reviews*, 60, 91–109. Available from: <https://doi.org/10.1016/j.quascirev.2012.10.037>
- Turner, T.E., Swindles, G.T. & Roucoux, K.H. (2014) Late Holocene ecohydrological and carbon dynamics of a UK raised bog: Impact of human activity and climate change. *Quaternary Science Reviews*, 84, 65–85. Available from: <https://doi.org/10.1016/j.quascirev.2013.10.030>
- van Kolfschoten, T. & Gibbard, P.L. (2000) The Eemian – local sequences, global perspectives: introduction. *Netherlands Journal of Geosciences*, 79, 129–133. Available from: <https://doi.org/10.1017/S0016774600021661>
- Vandenbergh, J. & van der Plicht, J. (2016) The age of the Hengelo interstadial revisited. *Quaternary Geochronology*, 32, 21–28. Available from: <https://doi.org/10.1016/j.quageo.2015.12.004>
- Veil, S., Breest, K., Höfle, H.-C., Meyer, H.-H., Plisson, H., Urban-Küttel, B. et al. (1994) Ein mittelpaläolithischer Fundplatz aus der Weichsel-Kaltzeit bei Lichtenberg, Lkr. *Lüchow-Dannenberg. Germania*, 72, 1–66.
- Velichko, A., Novenko, E., Pisareva, V., Zelikson, E., Boettger, T. & Junge, F. (2005) Vegetation and climate changes during the Eemian interglacial in central and eastern Europe: Comparative analysis of pollen data. *Boreas*, 34, 207–219. Available from: <https://doi.org/10.1080/03009480510012890>
- Velichko, A.A., Morozova, T.D., Nechaev, V.P., Rutter, N.W., Dlusskii, K.G., Little, E.C. et al. (2006) Loess/paleosol/cryogenic formation and structure near the northern limit of loess deposition, East European Plain, Russia. *Quaternary International*, 152–153, 14–30. Available from: <https://doi.org/10.1016/j.quaint.2005.12.003>
- Vogel, S., Märker, M., Rellini, I., Hoelzmann, P., Wulf, S., Robinson, M. et al. (2016) From a stratigraphic sequence to a landscape evolution model: Late Pleistocene and Holocene volcanism, soil formation and land use in the shade of Mount Vesuvius (Italy). *Quaternary International*, 394, 155–179. Available from: <https://doi.org/10.1016/j.quaint.2015.02.033>
- Voss, H.-H. (1981) Zur Geologie des Örings. *Veröffentlichungen der Urgeschichtlichen Sammlungen des Landesmuseums zu Hannover*, 26, 9–28.
- Weber, T. (1990) Paläolithische Funde aus den Eemvorkommen von Rabutz, Grabschütz und Gröbern. In: Eißmann, L. (Ed.) *Die Eemwärmzeit und die frühe Weichsel- Eiszeit im Saale-Elbe-Gebiet*, Geologie, Paläontologie, Palökologie. Altenburg: Naturkundliches Museum Mauritianum.
- Weiss, M. (2020) The Lichtenberg Keilmesser – it's all about the angle. Peresani M (ed). *PLoS ONE*, 15, e0239718. Available from: <https://doi.org/10.1371/journal.pone.0239718>
- Winsemann, J., Lang, J., Roskosch, J., Polom, U., Böhner, U., Brandes, C. et al. (2015) Terrace styles and timing of terrace formation in the Weser and Leine valleys, northern Germany: Response of a fluvial system to climate change and glaciation. *Quaternary Science Reviews*, 123, 31–57. Available from: <https://doi.org/10.1016/j.quascirev.2015.06.005>
- Woldstedt, P. (1956) Die Geschichte des Flußnetzes in Norddeutschland und angrenzenden Gebieten. *E&G Quaternary Science Journal*, 7, 5–12. Available from: <https://doi.org/10.3285/eg.07.1.01>
- Zagwijn, W. (1996) An analysis of Eemian climate in western and central Europe. *Quaternary Science Reviews*, 15, 451–469. Available from: [https://doi.org/10.1016/0277-3791\(96\)00011-X](https://doi.org/10.1016/0277-3791(96)00011-X)
- Żarski, M., Winter, H. & Kucharska, M. (2018) Palaeoenvironmental and climate changes recorded in the lacustrine sediments of the Eemian interglacial (MIS 5e) in the Radom Plain (central Poland). *Quaternary International*, 467, 147–160. Available from: <https://doi.org/10.1016/j.quaint.2016.12.001>

## SUPPORTING INFORMATION

Additional supporting information may be found in the online version of the article at the publisher's website.

**How to cite this article:** Hein, M., Urban, B., Tanner, D.C., Bunn, A.H., Tucci, M., Hoelzmann, P. et al. (2021) Eemian landscape response to climatic shifts and evidence for northerly Neanderthal occupation at a palaeolake margin in northern Germany. *Earth Surface Processes and Landforms*, 46 (14), 2884–2901. Available from: <https://doi.org/10.1002/esp.5219>